7-17-1964

Light sources for the excitation of resonance fluorescence in potassium and rubidium.

Robert J. Atkinson
University of Windsor

LIGHT SOURCES FOR THE EXCITATION OF RESONANCE FLUORESCENCE IN POTASSIUM AND RUBIDIUM

by

Robert J. Atkinson

A Thesis

Submitted to the Faculty of Graduate Studies through the Department of Physics in Partial Fulfillment of the Requirements for the Degree of Master of Science at the University of Windsor.

Windsor, Ontario

1964

ProQuest Information and Learning Company
789 East Eisenhower Parkway
P.O. Box 1346
Ann Arbor, MI 48106-1346

APPROVED

L. Krause

. . . . . .

Dr. L. Krause

E. Habib

. . . . . .

Dr. E. E. Habib

C. Kassimatis

. . . . . .

Dr. C. Kassimatis

ABSTRACT

The properties of newly developed potassium and rubidium spectral lamps have been systematically investigated in relation to their operating parameters. A comparison was made with two commercially available lamps, manufactured by Osram and Varian Associates, with respect to integrated intensity, peak intensity, half-width, and degree of self-reversal of the resonance lines. It was found that the radiofrequency sources, developed in this laboratory, emit potassium and rubidium resonance lines of significantly higher peak intensities and smaller half-widths than those produced by the other lamps. The degree of self-reversal in the resonance lines was also found to be very much more advantageous. Typical half-widths of the resonance lines of potassium and rubidium produced by the radiofrequency source were found to be 0.15 $cm.^{-1}$ and 0.37 $cm.^{-1}$ respectively, compared to the corresponding widths of 0.34 $cm.^{-1}$ and 1.5 $cm.^{-1}$ respectively emitted by the Osram lamp.

ACKNOWLEDGEMENTS

I would like to express my appreciation for the assistance granted me in the preparation of this thesis by Dr. L. Krause, under whose supervision this investigation was conducted, and for many helpful discussions with Dr. A. G. A. Rae and Mr. George Chapman. I gratefully acknowledge the financial assistance which was extended to me, in the form of a bursary, by the National Research Council of Canada.

TABLE OF CONTENTS

TABLE OF CONTENTS, CONTINUED

LIST OF TABLES

LIST OF DIAGRAMS

LIST OF DIAGRAMS, CONTINUED

CHAPTER I

INTRODUCTION

The investigation of atomic collisions in gases, utilizing the phenomenon of sensitized fluorescence, requires appropriate sources of light. The types of commercially available sources were found to be not satisfactory, mainly because they tend to produce spectral lines of excessive breadth and self-reversal. Therefore a new radiofrequency excited light source of the type described by Gerard (1961) was developed by Chapman (1963) for the purpose of exciting resonance fluorescence in alkali metals. This lamp was found to be superior to the spectral lamps manufactured by Osram Lamp Works (Germany) for the excitation of resonance fluorescence in potassium and rubidium vapours by Chapman (1963) and Rae (1963) at very low vapour pressures (less than 10^{-4} mm. Hg). It was felt necessary to carry out a systematic investigation of this lamp in comparison with the Osram lamp and with a commercial radiofrequency light source manufactured by Varian Associates of California.

Suitable sources for the excitation of resonance fluorescence must emit resonance lines with a high intensity and a small half-width. Some sources may have high integrated intensities but a large half-width so that the intensity at the centre of the spectral line is not very large. Several factors may contribute to line broadening. Doppler broadening arises from the thermal motions of the radiating atoms. The frequency of the light emitted may also be perturbed by collisions with neighbouring atoms, either of the same type or belonging to a foreign gas. If ions are present in large concentrations, their electric fields will also cause broadening of the emission lines through the Stark effect. In addition, the spectral lines may be self-reversed. When resonance light is emitted from a vapour lamp, it usually has to pass through a layer of unexcited

atoms before emerging to the outside. During this passage the light is absorbed by the unexcited atoms, which tend to absorb the centre of the resonance lines more strongly than the wings. The spectral lines which are finally emitted by the lamp are thus weakened in their centres. If they are less intense at the centre than in the wings they are said to be self-reversed. An additional intensity weakening factor, which arises in the case of alkali metal vapour lamps, is the chemical action of the vapour on the glass envelope. The alkali vapours attack pyrex glass to form an opaque brown deposit.

In the lamps which are commonly used for the production of atomic spectra, an ionic discharge is passed between two electrodes, with various methods being employed to reduce self-reversal and a darkening of the glass. Osram lamps are of the alternating current discharge type, manufactured from alkali-resistant glass, and the discharge section is placed in a vacuum envelope to reduce conduction of heat; a constant temperature throughout the discharge section should reduce self-reversal.

Houtermanns (1932) described a discharge lamp especially designed to reduce self-reversal. The central portion of the discharge tube is flattened to a thickness not exceeding 2 mm., so the the emitted light does not have to traverse a thick layer of vapour in emerging from the lamp. Ermisch and Seiwert (1959) attempted to use a sodium lamp of the Houtermanns' type made of sodium-resistant glass but were unsuccessful in that the lamps would crack after a short period of use. This was attributed to strains in the sodium-resistant glass which could not be properly annealed and to large temperature gradients in the glass when the lamp was operating.

Carlo and Lochte-Holtgreven (1927) designed a lamp in which the darkening of the exit window was prevented by passing a stream of inert

gas at a pressure of 3-5 mm. Hg from the anode, across the exit window, to a point near the cathode. The alkali vapour then occupies a small region near the cathode. The emission is viewed in the direction of the discharge current flow so that there is no unexcited vapour between the emitting layer and the exit window, and self-reversal should be slight. Hoffman and Seiwert (1960) investigated the potassium resonance fluorescence produced by this type of lamp and found that it emitted lines which were less self-reversed but also considerably less intense than those produced by an Osram lamp. Additional disadvantages of this type of lamp are its large size and the necessary system for the circulation of inert gases.

Hoffman and Seiwert also investigated the cataphoresis lamp designed by Druyvesteyn (1935) and found it to be superior to the Osram lamp in regard to degree of self-reversal. Cataphoresis consists of a migration of the positive metallic ions toward the cathode in a direct current discharge. The window of this lamp is placed on that side of the anode which is remote from the cathode and does not suffer darkening. This is perhaps the best type of alkali discharge lamp containg internal electrodes.

An electrodeless discharge in alkali vapours was used by Jackson (1928) to determine the hyperfine structure separations in cesium and later in rubidium (1933). The discovery of the techniques of optical pumping created a demand for high intensity sources of non-self-reversed alkali resonance lines. Bell, Bloom, and Lynch in 1959 developed the radiofrequency lamp manufactured by Varian, and Gerard (1962) gave the design for a lamp which could be constructed in the laboratory. The latter lamp also had the advantage that the vapour pressure in the discharge tube

and the radiofrequency power supplied could be controlled. Radiofrequency lamps of this type are being used in this laboratory for the excitation of resonance fluorescence in the vapours of potassium, rubidium, and cesium.

Osram spectral lamps, the Varian radiofrequency lamp, and the new radiofrequency lamp were investigated to determine the line intensities, half-widths, and degrees of self-reversal. When studying the profiles of spectral lines, it is necessary to use high resolution techniques, and use was made of a Hilger and Watts Fabry-Perot interferometer. It is hoped that the results of this investigation will be useful to workers in the field of atomic resonance fluorescence and related effects, and will provide a stimulus to further lamp development.

CHAPTER II

THE SHAPES OF THE RESONANCE SPECTRAL LINES OF POTASSIUM AND RUBIDIUM

The Structure of the Resonance Lines

If the free atoms of a gas are irradiated with light of a given frequency, the energy absorbed may raise atoms from the ground state (lowest energy level) to the energy level corresponding to the incident light frequency. This excited level is called a resonance level if the only allowed downward transition is directly to the ground state. Then the light emitted during this transition is of the same frequency as the incident light and is termed resonance radiation, and the spectral lines arising from such transitions are called resonance lines.

The electronic ground state of the alkali metals is a ^2S state ($\ell = 0$) and the first excited level is a ^2P ($\ell = 1$) state. In both cases the principal quantum number, n, is the same. The doublet structure arises from the splitting of the P level into two levels with spin and orbital angular momentum vectors parallel ($\ell + s = 1 + \frac{1}{2} = \frac{3}{2}$) or antiparallel ($\ell + s = 1 - \frac{1}{2} = \frac{1}{2}$). Since an atom can decay from the $^2P_{1/2}$ and $^2P_{3/2}$ levels only to the ground state, they are by definition resonance levels. In spectroscopic notation the transitions between the ground state and the two excited levels are represented by:

D_2 line: $n\,^2S_{1/2} \leftrightarrow n\,^2P_{1/2}$

D_1 line: $n\,^2S_{1/2} \leftrightarrow n\,^2P_{3/2}$

Each of the resonance spectral lines possesses several components called the hyperfine structure components, which arise in two ways. First, if there are several isotopes of the element present, their different nuclear masses and distributions of charge cause the resonance frequencies to be slightly shifted with respect to one another. This gives the sp-

pearance of a hyperfine structure. Secondly, the nuclear spin angular momentum vector $\vec{I}$ couples with the total electronic angular momentum vector $\vec{J}$ to form a set of hyperfine structure levels with quantum number F given by $F = I + J, I + J - 1, I + J - 2, - - - - - \left| I - J \right|$. There are $2I + 1$ or $2J + 1$ values of F, whichever is smaller. Transitions between these levels are governed by the selection rule $\Delta F = \pm 1, 0$ $(F = 0 \not\rightarrow 0)$ in conjunction with the usual selection rules for l and J: $\Delta l = \pm 1, \Delta J = \pm 1, 0$. The energies of these levels are given by:

$$E_F = E_J + \frac{A}{2}\left[F(F + 1) - I(I + 1) - J(J + 1)\right] \qquad (1)$$

where E_J is the energy of the original level, A is called the interval factor for hyperfine structure, and F, I, and J are quantum numbers. The energy intervals beween the levels within a hyperfine structure multiplet are governed by the interval rule and are in the ratio $(I + J):(I + J - 1):(I + J - 2) - - - -$. The hyperfine structure term diagrams of the $^2S_{1/2}$, $^2P_{1/2}$, and $^2P_{3/2}$ energy levels of K^{39}, Rb^{85} and Rb^{87} are given in Figures (1), (3), and (5). The hyperfine structures of the resonance lines which arise from the optically allowed transitions and their relative intensities are shown in Figures (2), (4), and (6). The energy splitting of the ground state is an order of magnitude larger than that of the P states. The intensity ratios of the components of each resonance line due to the ground state splitting depend only on the nuclear spin quantum number I, since the intensity ratios should be equal to the ratio of the statistical weights of the hyperfine structure levels of the ground state. The statistical weights are $2F + 1$, and their ratio is, for $J = \frac{1}{2}$, $\frac{I + 1}{I}$. This expression has the value $\frac{5}{3}$ for K^{39} and Rb^{87} which have $I = \frac{3}{2}$, and has the value $\frac{7}{5}$ in the case of Rb^{85} which has $I = \frac{5}{2}$.

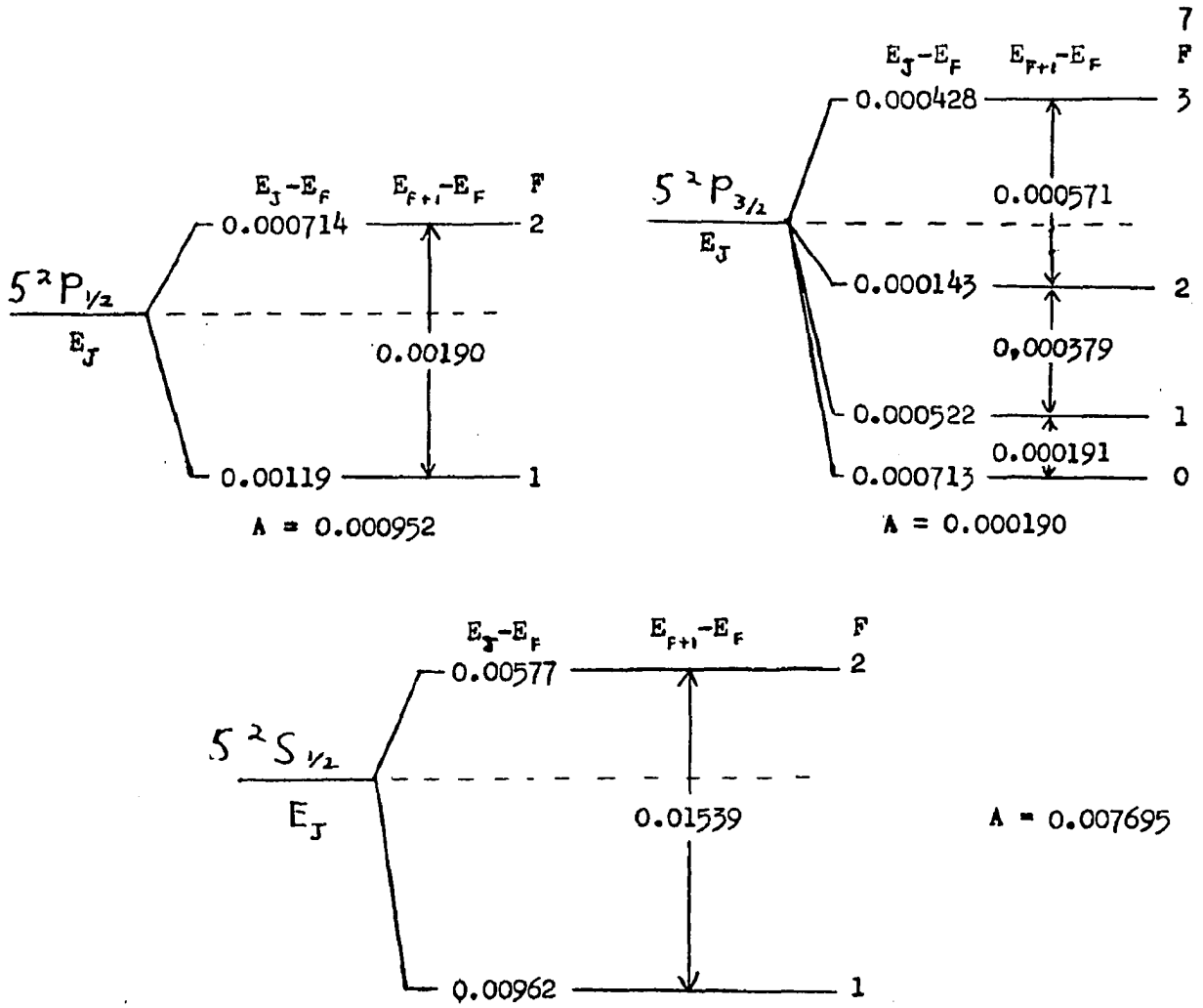

Figure (1) The Hyperfine Structure Term Diagrams of the $^2S_{1/2}$, $^2P_{1/2}$, and $^2P_{3/2}$ Energy Levels of Potassium^{39}

Note: All separations are in units of cm.$^{-1}$

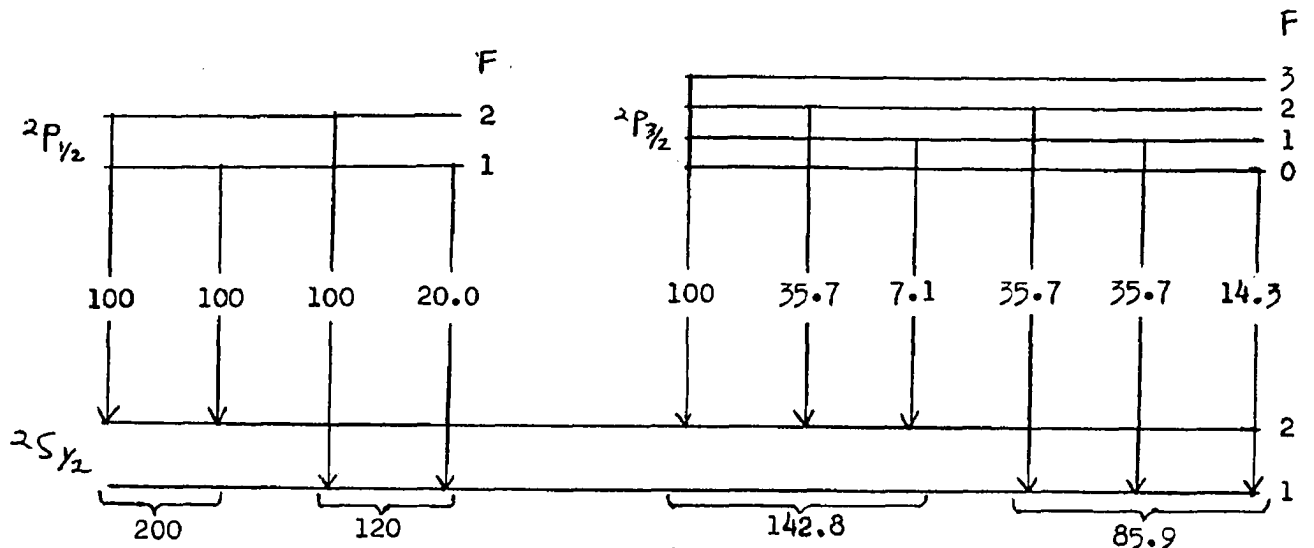

Intensity Ratios: $\frac{200}{120} = \frac{5}{3} = 1.67$; $\frac{142.8}{85.9} = \frac{5}{3} = 1.67$

Figure (2) Optically Allowed Transitions and Their Relative Intensities. Intensity Ratios of Components Due to Ground State Splitting.

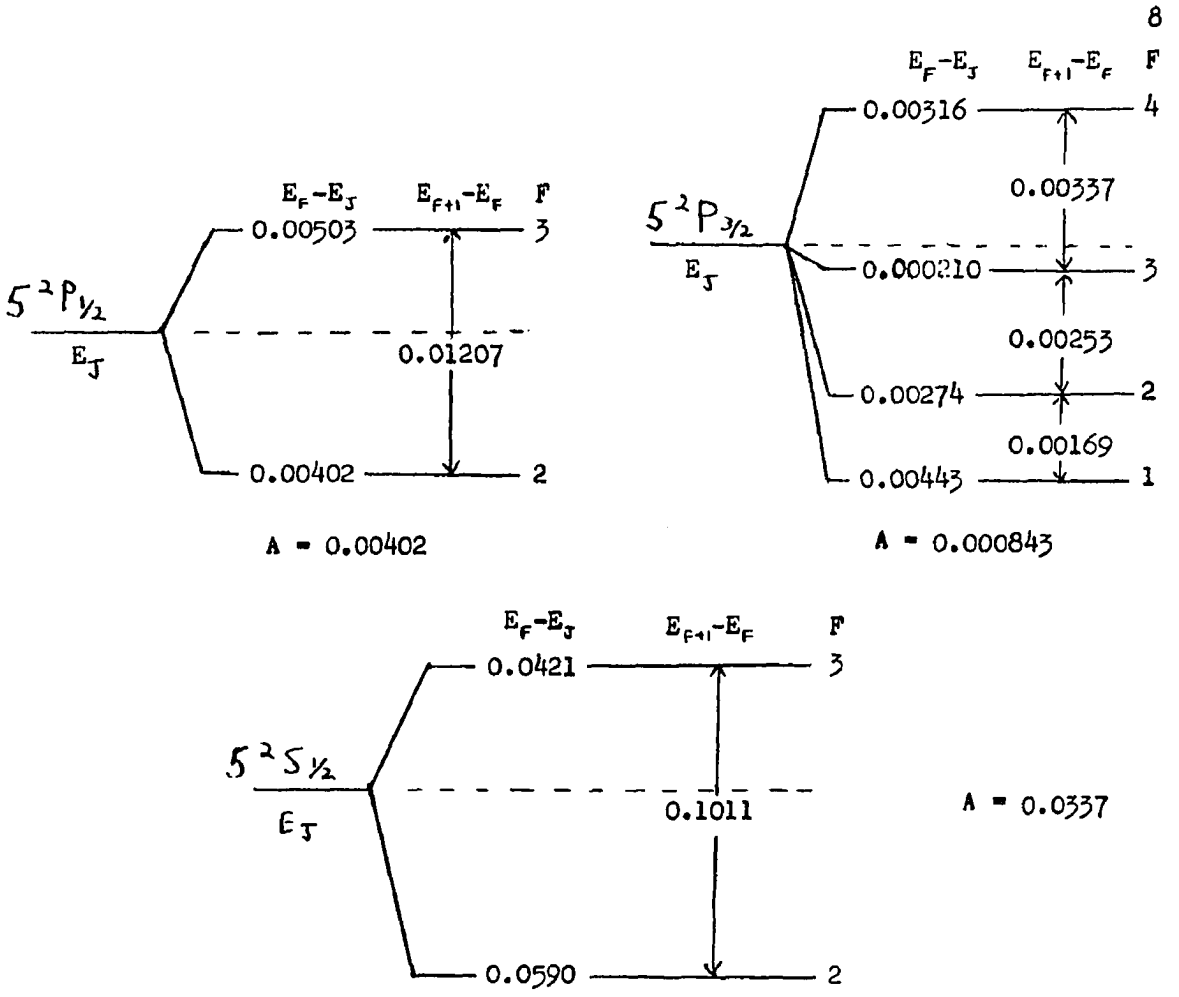

Figure (3) The Hyperfine Structure Term Diagrams of the $^2S_{1/2}$, $^2P_{1/2}$, and $^2F_{3/2}$ Energy Levels of Rubidium^{85}

Note: All separations are in units of cm.$^{-1}$

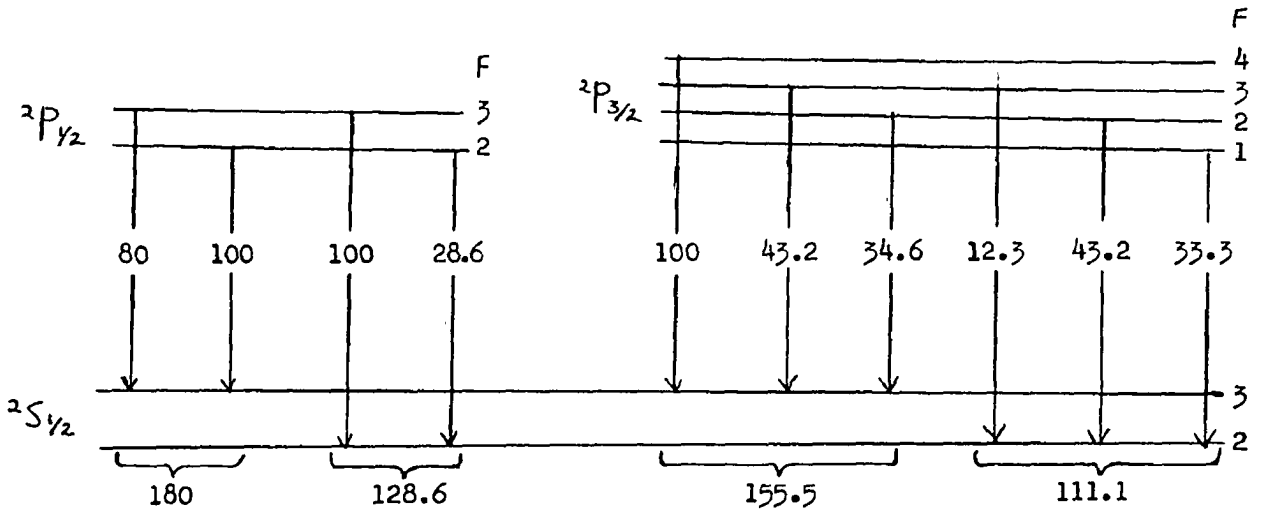

Intensity Ratios: $\frac{180}{128.6} = \frac{7}{5} = 1.40$; $\frac{155.5}{111.1} = \frac{7}{5} = 1.40$

Figure (4) Optically Allowed Transitions and Their Relative Intensities. Intensity Ratios of Components Due to Ground State Splitting.

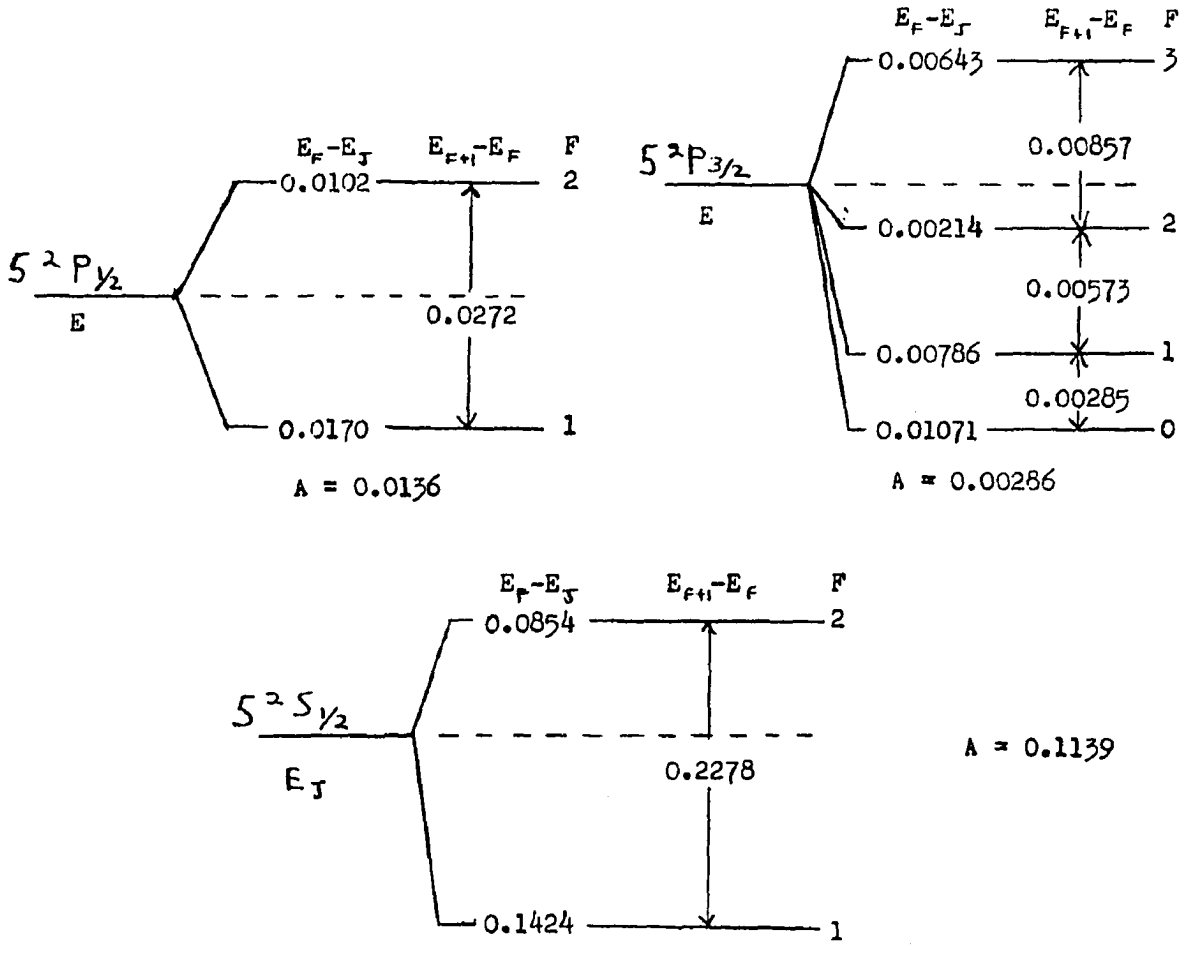

Figure (5) The Hyperfine Structure Term Diagrams of the $^2S_{1/2}$, $^2F_{1/2}$, and $^2P_{3/2}$ Energy Levels of Rubidium ^{87}

Note: All separations are in units of cm.$^{-1}$

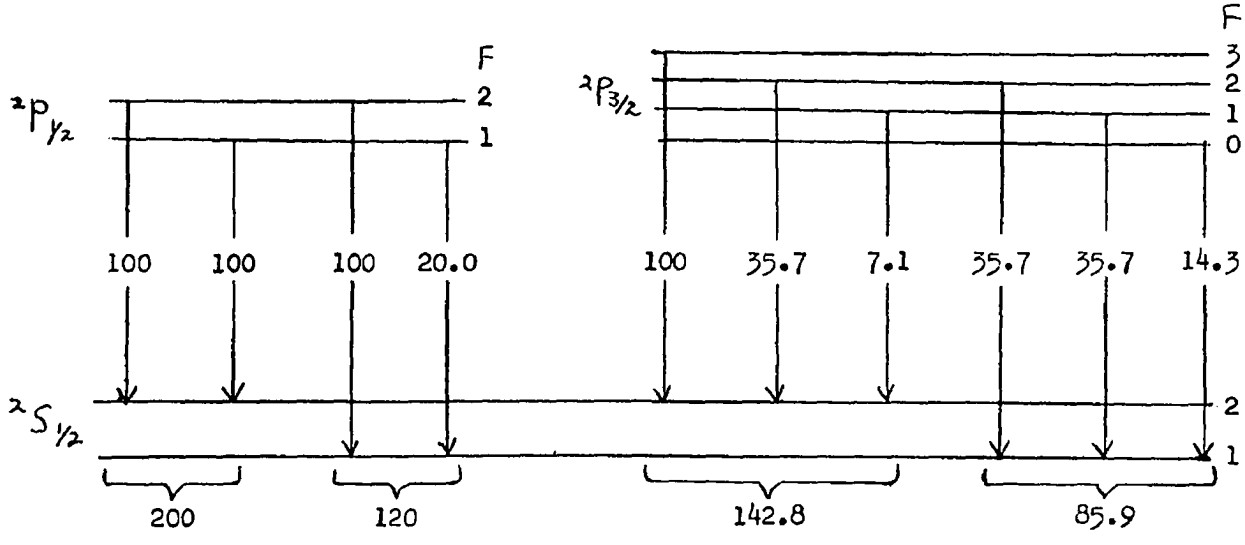

Intensity Ratios: $\frac{200}{120} = \frac{5}{3} = 1.67$; $\frac{142.8}{85.9} = \frac{5}{3} = 1.67$

Figure (6) Optically Allowed Transitions and Their Relative Intensities. Intensity Ratios of Components Due to Ground State Splitting.

Calculations of Intensity Profiles of Spectral Lines

The intensity distribution of emitted radiation may be derived theoretically assuming various broadening effects. The resonance distribution arises from the properties of the atomic energy levels themselves. Its shape may be preserved under other types of broadening, such as collision broadening, the only effect being an increase in width. The Doppler distribution arises from the apparent change in frequency of radiation emitted by moving atoms.

(i) Resonance Distribution of Frequencies

On the classical model, excitation of an atom occurs when the atom receives an impulse that displaces one or more electrons from their equilibrium positions. A displaced electron oscillates and radiates according to the laws of dipole radiation. The radiation represents a loss of energy and the electron executes a damped vibration. The oscillating electron is subject to an elastic restoring force, and to a radiation reaction force acting when the acceleration is changing. Because of the damping of the motion, the total radiated power decreases exponentially, with a time constant of the order of 10^{-8} seconds, which is called the average lifetime of the excited state of the atom. The shape of the spectral line is found by a Fourier analysis of the distribution of radiated flux density over the frequency range. The resonance distribution function is given by:

$$P_R(\nu) = \frac{1}{2\pi} \frac{\Delta\nu_R}{(\nu-\nu_0)^2 + \left(\frac{\Delta\nu_R}{2}\right)^2} \qquad (2) \quad \text{(Stone, 1963)}$$

where $\Delta\nu_R$, the corresponding half-width of the spectral line, is given by

$$\Delta\nu_R = \frac{4\pi e^2}{3mc^2} \nu_0^2 \text{ cm.}^{-1}$$

$$= 1.19 \times 10^{-12} \nu_0^2 \text{ cm.}^{-1} \qquad (3)$$

In quantum mechanics the natural line width arises from the fact that each of the two energy levels E_2 and E_1, between which the transition occurs, has a small uncertainty in its energy, ΔE_2 and ΔE_1, respectively. According to the theory of Weisskopf and Wigner (1930), the intensity distribution within the line is then given by:

$$F_R(\nu) = \frac{1}{2\pi} \frac{\Delta\nu_R}{(\nu-\nu_{21})^2 + (\Delta\nu_R/2)^2} \qquad (4)$$

where ν_{21} is the central frequency of the line: $\nu_{21} = \frac{E_2 - E_1}{h}$. This intensity distribution has the same form as the classical one, but the half-width is the sum of the frequency uncertainties corresponding to the uncertainties in the energy levels:

$$\Delta\nu_R = \frac{\Delta E_1}{h} + \frac{\Delta E_2}{h} = \frac{1}{2\pi\Delta t_1} + \frac{1}{2\pi\Delta t_2} \qquad (5)$$

using $\Delta E \Delta t \sim \hbar$. In this case Δt_1 is the lifetime of the level of energy E_1 against all spontaneous transitions to lower levels of energy E_K. The reciprocal of the lifetime of an energy level is the Einstein A coefficient, defined as the probability per second that a transition will occur from E_1 to E_K. Substituting for $\frac{1}{\Delta t_1}$ we have for level 1:

$$\frac{\Delta E_1}{h} = \frac{1}{2\pi} \left(\frac{8\pi^2 e^2}{mc^3}\right)\left(\sum_K \nu_{1K}^2 f_{1K}\right) \qquad (6)$$

where f_{1K} is called the oscillator strength corresponding to a transition from E_1 to E_K. A similar expression holds for all transitions from the level with energy E_2 to all lower levels with energy E_ℓ. Thus

$$\Delta\nu_R = \frac{4\pi e^2}{mc^3}\left(\sum_K \nu_{1K}^2 f_{1K} + \sum_\ell \nu_{2\ell}^2 f_{2\ell}\right) \qquad (7)$$

If the spectral line being considered is a resonance line, the lower state has no downward transitions, and so $f_{1K} = 0$, and $\frac{\Delta E_1}{h} = 0$. This may also be seen from the fact that the ground state has infinite lifetime and thus no uncertainty in energy. The expression for the half-width of the line reduces to:

$$\Delta\nu_R = \frac{4\pi e^2}{mc^3} f_{21} \nu_{21}^2 . \qquad (8)$$

(ii) Doppler Distribution of Frequencies (the Gaussian Distribution)

If an atom emits a light wave of actual frequency ν_o, and also has a component of velocity, v, along the direction of observation, the apparent frequency as seen by the observer is given by:

$$\nu = \nu_o \left(1 \pm \frac{v}{c}\right) . \qquad (9)$$

When a large number of atoms of mass M are in thermal equilibrium at an absolute temperature T, the probability P(v) that at a given time any one atom has a velocity along a given direction in the range v to v + dv, is:

$$P(v) = \left(\frac{M}{2kT}\right)^{\frac{1}{2}} \exp\left[-\frac{Mv^2}{2kT}\right] , \qquad (10)$$

where k is the Boltzmann constant. The Doppler distribution of frequencies is obtained by substituting in the above equation the expression for the velocity obtained from Equation (9):

$$P_D(\nu) = \left(\frac{Mc^2}{2kT}\right) \exp\left[-\frac{M}{2kT}\frac{c^2(\nu - \nu_o)^2}{\nu_o^2}\right] \qquad (11)$$

This equation describes the profile of a spectral line whose half-width is:

$$\Delta\nu_D = 2\left[\frac{2kT}{Mc^2} \ln 2\right]^{\frac{1}{2}} \nu_o \text{ cm.}^{-1}$$

$$= 7.1 \times 10^{-7} \sqrt{\frac{T}{M}}\, \nu_o \text{ cm.}^{-1}, \qquad (12)$$

where M is in atomic mass units.

(iii) Lorentz Collision Broadening Theory

This theory, developed mainly by Lorentz (1906), is based on the assumption that an atom radiates continually during the time between two collisions with other atoms, and that each collision stops the radiation process completely, the energy of vibration being converted into kinetic energy. If T is the time between collisions, the emission consists of a series of wave trains of finite length cT. A Fourier analysis of this type of emission yields the Lorentz formula for the

intensity distribution:

$$F_L(\nu) = \frac{1}{2\pi} \frac{\Delta\nu_L}{(\nu-\nu_0)^2 + \left(\frac{\Delta\nu_L}{2}\right)^2} \qquad (13)$$

This distribution has the same form as the natural spectral line, and has a half-width given by:

$$\Delta\nu_L = \frac{1}{\pi\tau} \qquad (14)$$

where τ is the mean time between collisions. It can by shown that the half-width of a line broadened by natural damping and Lorentz or collision broadening is the sum of the half-widths due to the two separate effects. The quantity $1/\tau$ is the number of collisions per second, which is known from gas kinetic theory to be $\pi\rho^2\bar{v}n$, where ρ is known as the optical collision diameter, which is the average distance between the centres of two colliding atoms at which radiation stops, $\bar{v}$ is the average colliding velocity of the atoms, and n is the volume density of atoms. The half-width of the spectral line then becomes:

$$\Delta\nu_L = \rho^2 \bar{v}\, n \qquad (15)$$

The kinetic theory of gases yields

$$\bar{v} = \sqrt{\frac{8\,kT}{\pi\mu}} = 1.46 \times 10^4 \sqrt{\frac{T}{\mu}} \qquad (16)$$

where μ is the reduced mass of the colliding atoms. From the ideal gas law it may be shown that

$$n = 9.64 \times 10^{18} \frac{P}{T} \frac{\text{atoms}}{\text{cc.}} \qquad (17)$$

Substitution of these values into Equation (15) yields

$$\Delta\nu_L = 4.70 \times 10^{12} \frac{P\rho^2}{\sqrt{\mu T}} \text{ cm.}^{-1} \qquad (18)$$

This derivation makes no assumptions regarding the force law between the colliding particles. However the ranges of the various forces involved are reflected in the magnitudes of the optical collision diameters. The perturbing forces between like particles are much greater than those between unlike atoms, and so the collision diameters for self-pressure

broadening are larger than those for pressure of foreign gases. The optical collision diameters for broadening of the resonance lines of the alkali metals have been determined experimentally and are given in Table (1).

In the case of broadening by foreign gases, the coupling between atoms is chiefly due to forces of the van der Waals type. London (1930) gave quantum mechanical formulae for the additional energies of the excited and the ground levels of the radiating atom due to foreign gas perturbers. The perturbation energy varies as $\frac{1}{r^6}$, where r is the distance between the two atoms, and the change in the frequency emitted is given by:

$$\nu - \nu_0 = b \sum_i \frac{1}{r_i^6}; \qquad b \approx 10^{-21} \text{ cm.}^5 \qquad (19)$$

Weisskopf (1932) defined the optical collision diameter as the distance of separation between two atoms at which the phase of the radiation has undergone a change of about 1 radian, and obtains a half-width

$$\Delta\nu = 2.2\, b^{2/5} \bar{v}^{3/5} n \text{ cm.}^{-1} \qquad (20)$$

The resonance perturbation energies between like atoms arise from the exchange of excitation energy (light quantum) between one another without accompanying radiation, and vary as $\frac{1}{r^3}$. This possibility of the transfer of excitation energy reduces the lifetime of the excited state, and from the uncertainty principle, any reduction in lifetime corresponds to an increase in the uncertainty of the energy and a broadening of the line emitted. The change in frequency emitted is

$$\nu - \nu_0 = \frac{e^2 f_{12}}{8 \pi^2 m \nu_0} \frac{1}{r^3} \qquad (21)$$

In this case, Weisskopf obtains

$$\Delta\nu = \frac{e^2 f_{12}}{2 \pi m \nu_0} n \text{ cm.}^{-1} \qquad (22)$$

Weisskopf's formulae show the same linear variation with n as the Lorentz formula, which has been widely verified experimentally, and also yield optical collision diameters in agreement with the experimental values.

(iv) Stark Broadening

In this case the perturbing atoms carry permanent electric fields which may be due to ions, dipoles, or multipoles. The largest fields are produced by ions. Holtsmark (1919) calculated the spectral line width produced by a broadening of the energy levels through the Stark effect. This theory is based on the determination of a probability function for the existence of a particular field at the emitter. The intensity distribution of radiation is given by

$$P_S(\nu) = \int_0^\infty P_S(E, \nu)\, W(E)\, dE \qquad (23)$$

where $P(E,\nu)$ is the intensity distribution in a line broadened by the field E, and W(E) is the field strength probability function. The expressions W(E) are found to be infinite series or integrals which must be evaluated numerically. For broadening by dipoles, the intensity distribution is of the resonance form, with a half-width proportional to the dipole moment and to the volume density of the perturbers. In the case of broadening by ions the intensity distribution is an integral function, but it is very nearly of the Gaussian shape, as indicated by comparison of the line profiles given in Figure (7). The half-width for broadening by ions is given by

$$\Delta\nu_S = C\, e\, n^{2/3} \qquad (24)$$

where C is a constant, e is the ionic charge, and n is the volume density of ions. This expression has been verified experimentally. (See the review by Margenau and Watson, 1936)

Table (2) gives a summary of the sources of line broadening of the potassium and rubidium resonance lines.

Table (1) Optical Collision Diameters

Type of Collision	Optical Collision Diameter	Source
K - K	200 Å	Lloyd and Hughes, 1937
K - A	14.4Å	Hull, 1936
Rb - Rb	200 Å	Ch'en, 1940
Rb - A	13.4Å	Ch'en, 1940

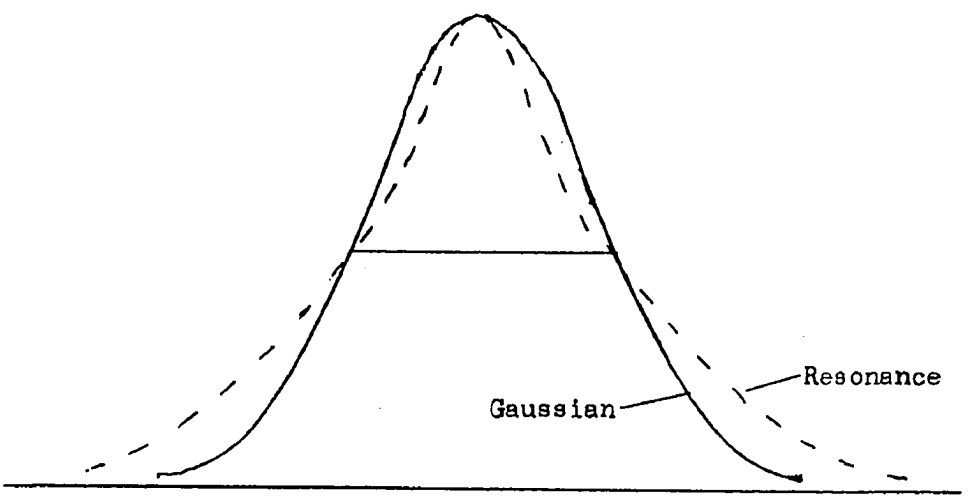

Figure (7a) Comparison of Resonance and Gaussian Distributions

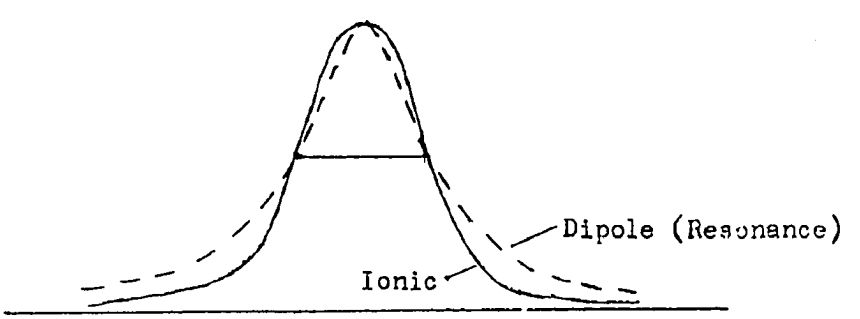

Figure (7b) Comparison of Stark Theory Line Shapes.

Table (2) Calculated Values of Half-widths of Potassium and Rubidium Resonance Lines

Cause of Broadening	Half-widths in $cm.^{-1}$			
	7665 Å Line (K)	7699 Å Line (K)	7800 Å Line (Rb)	7948 Å Line (Rb)
Natural Line Width	0.015600	0.015600	0.22800	0.22799
Doppler Broadening at 250°C	0.0493	0.0491	0.2499	0.2504
Collision with Argon at a Pressure of 2 mm. Hg	0.0194	0.0173	0.2565	0.2292
Collisions with Like Atoms at 1 mm. Hg pressure	0.287	0.203	0.500	0.353
at 0.5 mm. Hg pressure	0.154	0.109	0.410	0.290
at 0.1 mm. Hg pressure	0.0485	0.0342	0.340	0.240
at 0.01 mm. Hg pressure	0.0245	0.0173	0.324	0.229

The components of each line due to ground state splitting are considered as being broadened separately. Thus the half-widths are the combination of the half-width of each hyperfine component and the ground state splitting, which is 0.0154 $cm.^{-1}$ in the case of potassium and 0.2278 $cm.^{-1}$ in the case of rubidium.

The broadening by argon is greater by a factor of 1.12 for the short wavelength component. (Ch'en, 1957)

Foley (1946) has calculated the quantum mechanical resonance interaction between the degenerate sub-levels of an excited energy level with those of a like atom, and has found that the short wavelength component should have a half-width greater by a factor of $\sqrt{2}$ under self-pressure broadening, which has been verified experimentally by the workers referred to in Table (1).

The Theory of Self-Absorption

Let us consider a spectral line with frequency ν_o at the centre and Intensity distribution I (ν), and let the radiation be propagated with velocity c in the +X direction. Then the intensity absorbed per unit distance dx will be proportional to the initial intensity distribution, and to the profile of the absorption line, $F_a(\nu)$.

$$\frac{dI(\nu)}{dx} = \frac{dI(\nu)}{c\,dt} = -k\,F_a(\nu)\,I(\nu) \qquad (25)$$

The constant of proportionality, k, is evaluated by considering the absorption from a continuous spectrum where the energy of radiation per unit volume, ρ, is independent of the frequency ν. In this case the rate of energy absorption is:

$$\frac{dE}{dt} = -k\,c\left[\int_o^\infty F_a(\nu)\,d\nu\right] = -k\,c\,\rho \qquad (26)$$

The above is valid if $F_a(\nu)$ is normalized with respect to frequency so that $\int_o^\infty F_a(\nu)\,d\nu = 1$. Alternatively, the rate of absorption may be written as

$$\frac{dE}{dt} = n_a(x)\,B\,\rho\,h\nu_o \qquad (27)$$

which is the product of the rate of occurence of the absorptive transitions, $n_a(x)\,B\,\rho$, and the energy absorbed per transition, $h\nu_o$. $n_a(x)$ is the volume density of atoms capable of absorption and B is the Einstein absorption coefficient, the probability that an atom will undergo an absorptive transition per second. Equating (26) and (27),

$$k = -\frac{n_a(x)\,B\,h\nu_o}{c} \qquad (28)$$

Substitution in Equation (25) yields

$$\frac{dI(\nu)}{I(\nu)} = -\frac{h\nu_o\,B\,n_a(x)}{c}\,F_a(\nu)\,dx\,. \qquad (29)$$

If the light is emitted from a small volume at x_o, the intensity at the point x is found by integrating over x from x_o to x:

$$I(\nu, x) = I_0 P_e(\nu, x_0) \exp\left[-\frac{h\nu_0 B}{c} P_a(\nu) \int_{x_0}^{x} n_a(x)\, dx\right]. \quad (30)$$

$I_0 P_e(\nu, x_0)$ is the intensity distribution at x_0, where the light has not passed through any absorbing layers. I_0 is the peak intenity of the unabsorbed line and $P_e(\nu, x_0)$ is the intensity profile of the emitted radiation. In practically all cases the emission and absorption profiles have the same shape. In this case,

$$I(\nu, x) = I_0 P(\nu) \exp\left[-\frac{h\nu_0 B}{c} P(\nu) \int_{x_0}^{x} n_a(x)\, dx\right] \quad (31)$$

$$= I_0 P(\nu) \exp\left[-p \frac{P(\nu)}{P(\nu_0)}\right], \quad (32)$$

where $$p = \frac{h\nu_0 B}{c} P(\nu_0) \int_{x_0}^{x} n_a(x)\, dx. \quad (33)$$

p is termed the absorption parameter. Equation (32) gives the effect of absorption on the intensity I_0 emitted within an element of volume at x_0. It is necessary to further integrate it over the density of emitting atoms across the source, $n_e(x)$:

$$I(\nu) = I_0 P(\nu) \int_0^{\infty} n_e(x)\, dx \exp\left[-p \frac{P(\nu)}{P(\nu_0)}\right] \quad (34)$$

It may be seen that the shape and intensity of a spectral line emerging from a vapour source depend on three factors:

(i) the distribution function $P(\nu)$ which represents the line shape for negligible absorption,

(ii) the absorption parameter p which is a function of the amount of absorbing vapour that the light has to traverse and the probability of absorption,

(iii) the densities of emitting and absorbing atoms.

If self-reversal is present $I(\nu)$ will have two maxima, which are found by differentiating equation (34). It may be shown (Cowan and Dieke, 1948) that, if the densities of emitting and absorbing atoms are constant throughout the source, self-reversal is not possible. If there

is a maximum in the density of excited atoms at some point, $I(\nu)$ has maxima when the following condition is satisfied:

$$p \frac{F(\nu)}{F(\nu_0)} = 1 \qquad (35)$$

The intensity at the centre of the spectral line is, from Equation (34),

$$I(\nu_0) = I_0 F(\nu_0) \int n_e(x)\, dx \quad e^{-p}. \qquad (36)$$

The intensities of the two maxima are obtained by substituting Equation (35) into Equation (34):

$$I_{max} = I_0 \frac{F(\nu_0)}{p} \int n_e(x)\, dx \quad e^{-1}. \qquad (37)$$

Then

$$\frac{I_{max}}{I(\nu_0)} = \frac{e^{-1}}{p} \frac{1}{e^{-p}} = \frac{e^{p-1}}{p} \qquad (38)$$

which is independent of the form of $F(\nu)$, and allows the value of p to be determined experimentally. Self-reversal occurs for p greater than 1.

Substitution of the Gaussian distribution, Equation (11), into equation (35) yields:

$$\frac{(\delta\nu)^2}{(\Delta\nu_D)} = \frac{\ln p}{\ln 2} = \frac{\ln p}{0.693}, \qquad (39)$$

where $\delta\nu$ is the separation of the self-reversal maxima. If the width of the unabsorbed line, $\Delta\nu$, does not change as the absorption increases, a plot of $(\delta\nu)^2$ vs. p will have the same shape as a logarithmic curve of the form $(\delta\nu)^2 =$ (const.) x ln p.

Similar substitution of the resonance distribution, Equation (2), yields

$$\frac{(\delta\nu)^2}{(\Delta\nu_R)^2} = p - 1. \qquad (40)$$

If the resonance half-width remains constant as the line is absorbed, then a plot of $(\delta\nu)^2$ vs. p will be linear.

It is seen that, for either distribution, the separation of the reversal peaks equals the original half-width when p = 2. Then from Equation (38), $\frac{I_{max}}{I(\nu_0)} = 1.36$, or the intensity of the central minimum is 73.5% of the intensity of the peaks.

Using Equation (32), the following table may be constructed, giving the reduction in the intensity at the centre of a spectral line under varying degrees of absorption.

Table (3) Relative Intensities of Spectral Lines as Self-absorption Increases

Absorption Parameter p	$I(\nu)$	$\frac{I_{max}}{I(\nu_0)}$	$\frac{I(\nu_0)}{I_{max}}$
0	1.0		
0.5	0.607		
1.0	0.368		
1.5	0.223	1.10	91.0%
2.0	0.135	1.36	73.5%
2.5	0.081	1.78	56.0%

These values do not take into account the number of emitting atoms. In an actual source, the emission will increase with the absorption and the centre of the line will not decrease in intensity as rapidly as the above table indicates.

CHAPTER III

THE THEORY OF THE FABRY-PEROT INTERFEROMETER

This interferomter was developed by Fabry and Perot in 1897. It consists of a pair of plane parallel plates coated with a partially transparent layer of a highly reflecting metal. Fringes are produced in the transmitted light after multiple reflections in the air film between the plates. The transmitted intensity is given by Airy's formula:

$$I_t = \frac{T^2 I_o}{1 - 2R\cos\delta + R^2} , \qquad (41)$$

where R and T are the fractions of intensity reflected and transmitted, respectively, I_o is the intensity of the incident beam, and δ is the phase shift between successive reflected beams. The intensity is a maximum when $\cos\delta = 1$, or $\delta = 2n\pi$. In terms of the wavelength, λ, of the light, and the distance, t, between the reflecting surfaces, a transmitted intensity maximum occurs whenever

$$n\lambda = 2t\cos\theta , \qquad (42)$$

where n is the order of interference and θ the angle of incidence and emergence. This basic equation may also be written

$$n = 2\nu t\cos\theta , \qquad (43)$$

where ν is the frequency of the light in $cm.^{-1}$. All the light incident along a cone of semi-angle θ contributes to form a single circular fringe of angular radius θ. Near the centre of the fringe system, where θ is small,

$$n = 2\nu t . \qquad (44)$$

The change in frequency, $d\nu$, corresponding to a small change in order, dn, is given by

$$d\nu = \frac{dn}{2t} . \qquad (45)$$

The spectral range is defined as the frequency separation between two components whose orders differ by unity. The frequency separation of a

pair of components is found by determining their fractional orders, ϵ_1 and ϵ_2, and then using Equation (45). It may be shown from Equation (42) that the angular radius of the p-th fringe is given by

$$\theta_p = \sqrt{\frac{\lambda}{t}(\epsilon_1 + p - 1)} . \quad (46)$$

The p-th and (p + 1)-th fringes are connected by the following relation:

$$\epsilon_1 = \frac{\theta_{p+1}^2}{\theta_{p+1}^2 - \theta_p^2} - p = \frac{t\,\theta_{p+1}^2}{\lambda} - p . \quad (47)$$

In terms of the linear diameters, D, of the fringes,

$$\epsilon_1 = \frac{t\,D_{p+1}^2}{4 f^2 \lambda} - p , \quad (48)$$

where f is the effective focal length of the lens system used in focussing the fringes on the photographic plate. Similarly, if d_{p+1} is the linear diameter of the (p + 1)-th fringe arising from the second component,

$$\epsilon_2 = \frac{t\,d_{p+1}^2}{4 f^2 \lambda} - p . \quad (49)$$

It has been assumed that the two components are close enough that $\lambda_1 \approx \lambda_2 \approx \lambda$. Then the difference between the orders of the two components is

$$dn = \epsilon_1 - \epsilon_2 = (D_{p+1}^2 - d_{p+1}^2)\frac{t}{4 f^2 \lambda} \quad (50)$$

and the corresponding frequency separation is

$$d\nu = \frac{dn}{2t} = (D_{p+1}^2 - d_{p+1}^2)\frac{1}{8 f^2 \lambda}$$

$$= (D_{p+1}^2 - d_{p+1}^2) \times (\text{const.}) . \quad (51)$$

Obtaining expressions for D_{p+1} and D_p from Equation (48) it may be shown that

$$\frac{1}{8 f^2 \lambda} = \frac{1}{2 t (D_{p+1}^2 - D_p^2)} \quad (52)$$

Thus the constant in Equation (51) is a function of the interferometer spacing and the linear diameters of the fringes, and so it may be found by measuring the diameters of sets of fringes obtained with known values of t, the mirror spacing. An accurate value of this constant can be

determined for each wavelength under investigation, and thereafter it is not necessary to know the precise value of the mirror spacing, but only to obtain the differences in the squares of the diameters of the rings in order to calculate frequency separations.

CHAPTER IV

DESCRIPTION OF THE APPARATUS

The apparatus used to study the spectral line shapes is shown in Figure (8). It consisted of: the particular light source under investigation, a monochromator to isolate the resonance line being studied, a Fabry-Perot interferometer, a camera equipped with a shutter of variable aperture, and the necessary collimating and focussing lenses.

For purposes of determining the relative intensities of the spectral lines, a photomultiplier tube would be placed following the exit slit of the monochromator instead of the interferometer.

Alkali Metal Spectral Lamps

(i) Osram Spectral Lamps

Osram Spectral Lamps are alternating current discharge lamps. The electrodes, an inert gas which acts as a carrier of the discharge, and a small amount of the alkali metal are contained within a glass bulb. This bulb is enclosed in an outer envelope which serves as a mechanical cover and as a barrier against heat loss. The recommended operating current is 1.5 amperes, supplied at a voltage of 10 volts. It is well known that these lamps emit broad, self-reversed spectral lines.

(ii) The Varian Spectral Lamp

This lamp, manufactured by Varian Associates of California, is of the electrodeless, radiofrequency-excited type. It has been described by Bell, Bloom, and Lynch. (1961)

The radiofrequency oscillator circuit is of the push-pull type, operates at a frequency of 100 mc/sec., and produces a power dissipation of 3.75 watts. It is shown in Figure (9).

The bulb containing the alkali vapour is a sphere of diameter 1 cm. with a wall thickness of 0.2 mm., and has a small tip which serves

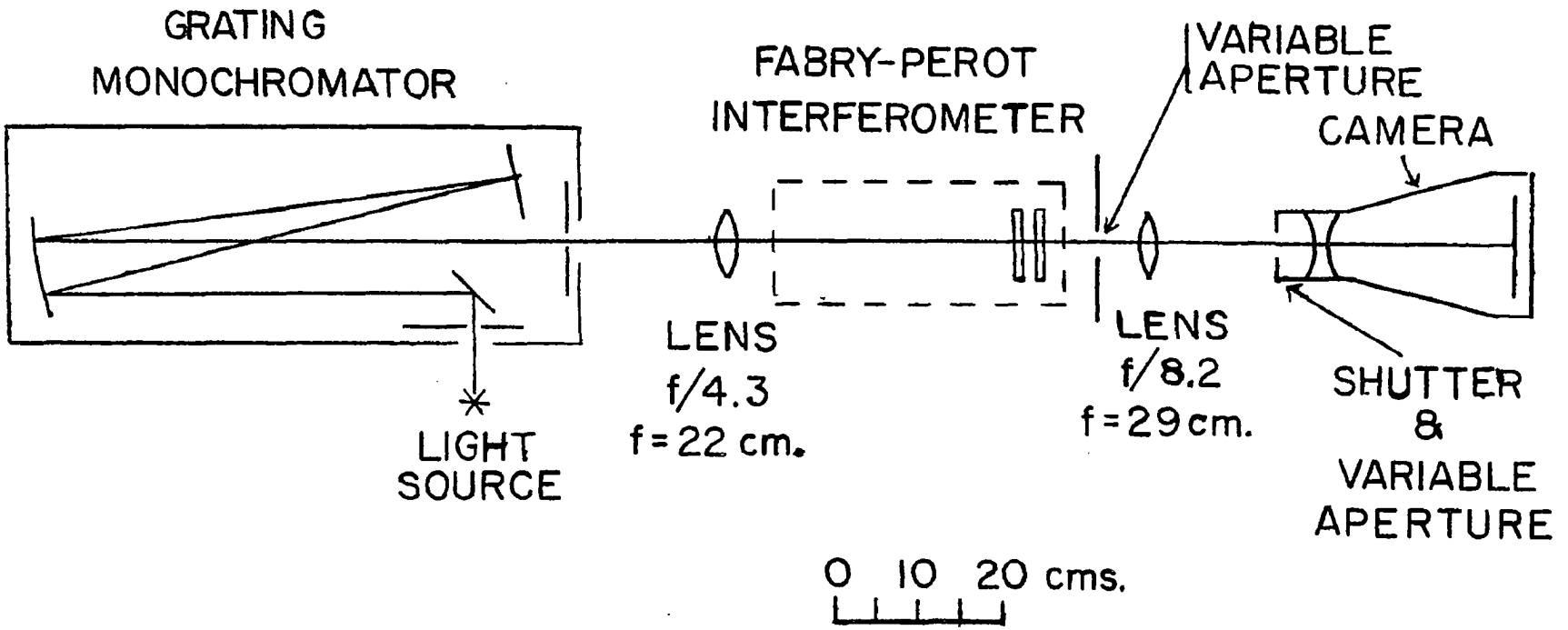

Figure (8) Apparatus Used to Study the Spectral Line Shapes

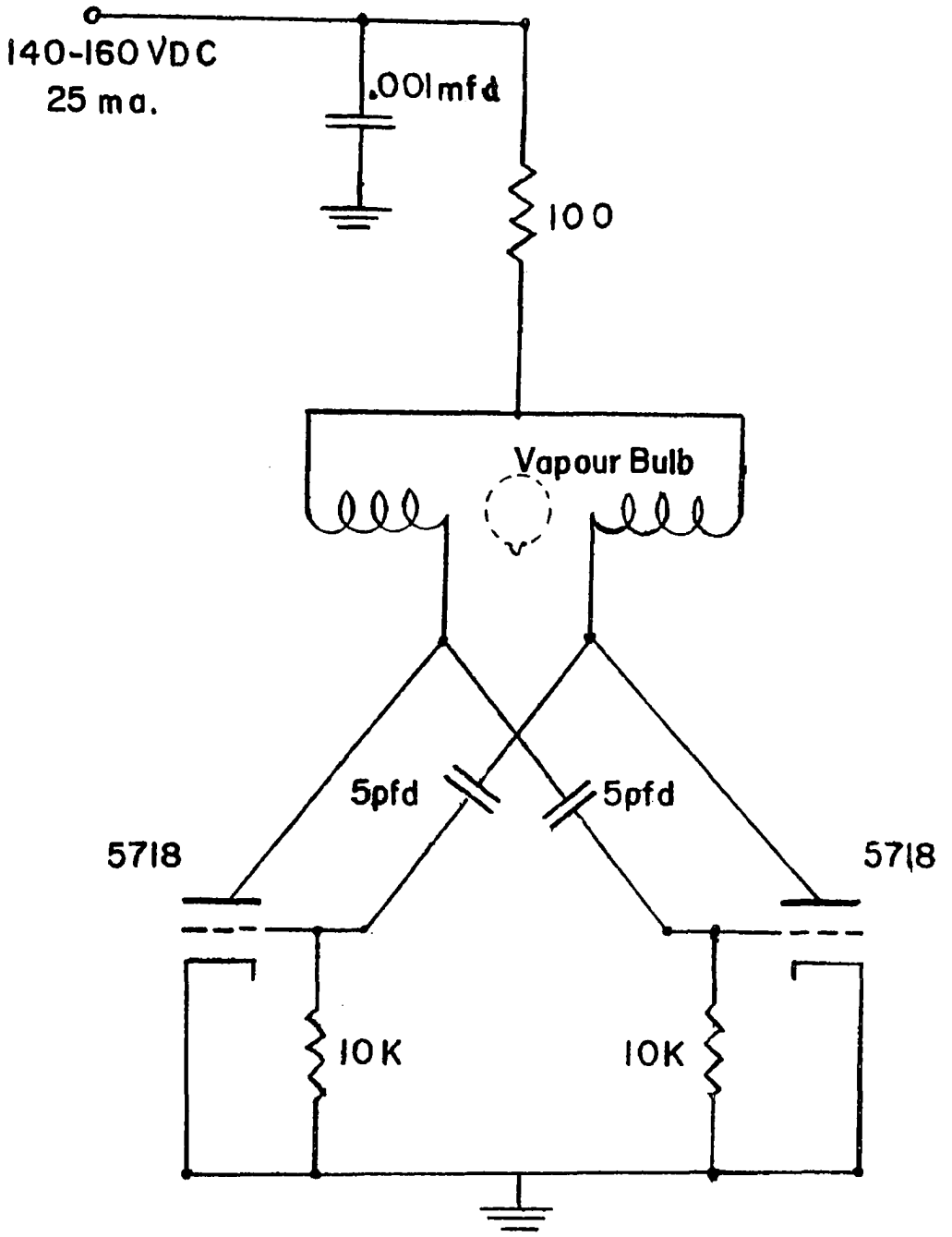

Figure (9) The Varian Lamp Oscillator Circuit

as a reservoir for the alkali metal. The operating temperature of the reservoir is 90°C and that of the bulb surface is 120°C. The carrier gas is krypton at a pressure of 1.6 mm. Hg. It has been chosen by the manufacturers because it apparently provides a more stable discharge than other inert gases.

(iii) The New Radiofrequency Lamp

The radiofrequency lamp used in this investigation was of the type described by Chapman (1963). The oscillator circuit was of a push-pull type operated in class C. Power was supplied by a Lambda Voltage-Regulated Power Supply Model C-482M. The frequency of about 60 mc/sec. was determined by the tank circuit and could be varied slightly by means of the trimmer capacitors. Power to the coil was regulated by a 10K potentiometer which controlled the current to the screen grids. The power dissipation of the plate circuit was about 100 watts and that of the screen grids about 5 watts. As the vapour pressure in the discharge tube increased, the impedance was lowered and the power dissipation also increased. However, in the experimental runs, the power dissipated in the plate circuit was held constant by adjusting the current to the screen grids. Figure (10) shows the circuit.

The electrodeless discharge was confined to a pyrex glass cylinder of length 6 cm. and diameter 1.8 cm., which contained about 0.5 gm. of the alkali metal, purified by vacuum distillation, and about 2.0 torr of argon gas to carry the discharge at low vapour densities of the metal. The vapour was coupled to the radiofrequency field by placing the bulb within the coil of the oscillator tank circuit. The base of the lamp acted as a reservoir for the metal and was heated to control the vapour pressure of the metal. The heater consisted of 3.3 ohms of #28 Chromel "A" heating wire in the form of a coil which was wrapped about the base of the lamp and was buried in an asbestos block. The heater current was regulated by a tran-

sistorized controller employing a thermistor as a sensing element. A chromel-alumel thermocouple was placed in contact with the glass of the reservoir. The temperature measured by this thermocouple could be varied from 70°C to over 200°C. A minimum lamp base temperature of slightly less than 70°C was obtained with zero heater current. This was caused by the dielectric heating effect which raises the temperature of the glass envelope within the radiofrequency coil to well over 200°C. Figure (11) shows the controller circuit.

The Monochromator

The monochromator was a Bausch and Lomb grating instrument, containing a 1200 line/mm. plane replica grating blazed at 7500 Å in the first order. The reciprocal linear dispersion of this instrument was 16 Å/mm. A slit width of 1.75 mm. was found sufficient to resolve the potassium resonance doublet.

The Interferometer

The Fabry-Perot interferometer was the Hilger and Watts Model N200 instrument. It contains an accurate screw of 1.0 mm. pitch, by means of which the gap between the mirrors can be varied continuously. The circular mirrors have aluminized surfaces and have diameters of 2.5 cm. Coarse and fine adjustments for parallelism of the mirrors are provided. The separation of the mirrors is measured with a linear millimetre scale in conjunction with a rotating disc calibrated in 0.01 mm. units. This scale,however, has a large zero error, which is dependent also on the positions of the mirrors in their retaining rings. Therefore the separation between the mirrors was measured with a travelling microscope, also calibrated in 0.01 mm. units.

The camera used was the Hilger and Watts Model D72 spectrometer camera, which accepts $4\frac{1}{4}$" x $3\frac{1}{4}$" photographic plates. This camera has mounted in it a concave lens and it was necessary to place a convex achromatic lens of focal length 29 cm. between it and the interferometer in order to

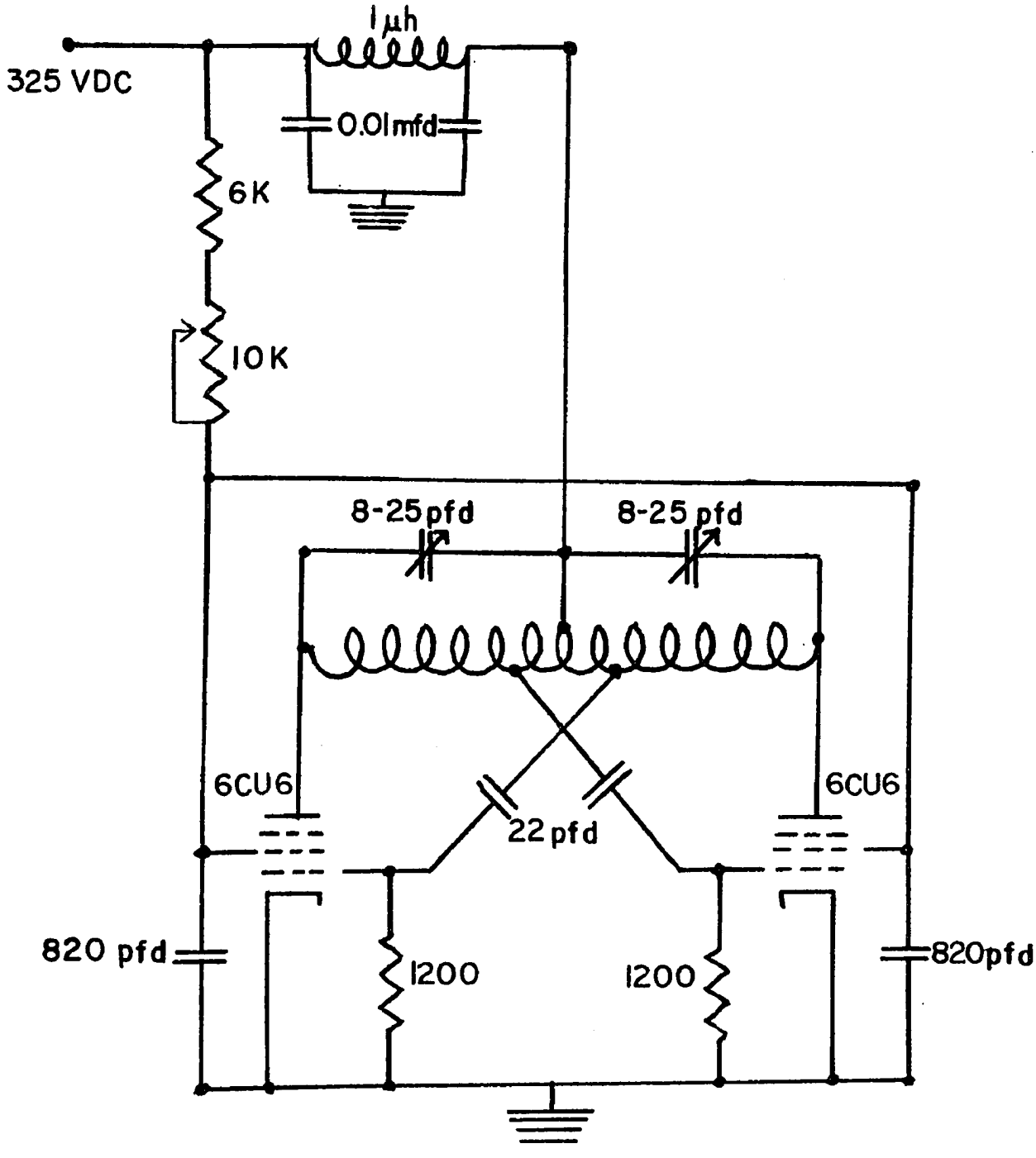

Figure (10) The New Radiofrequency Lamp Oscillator Circuit

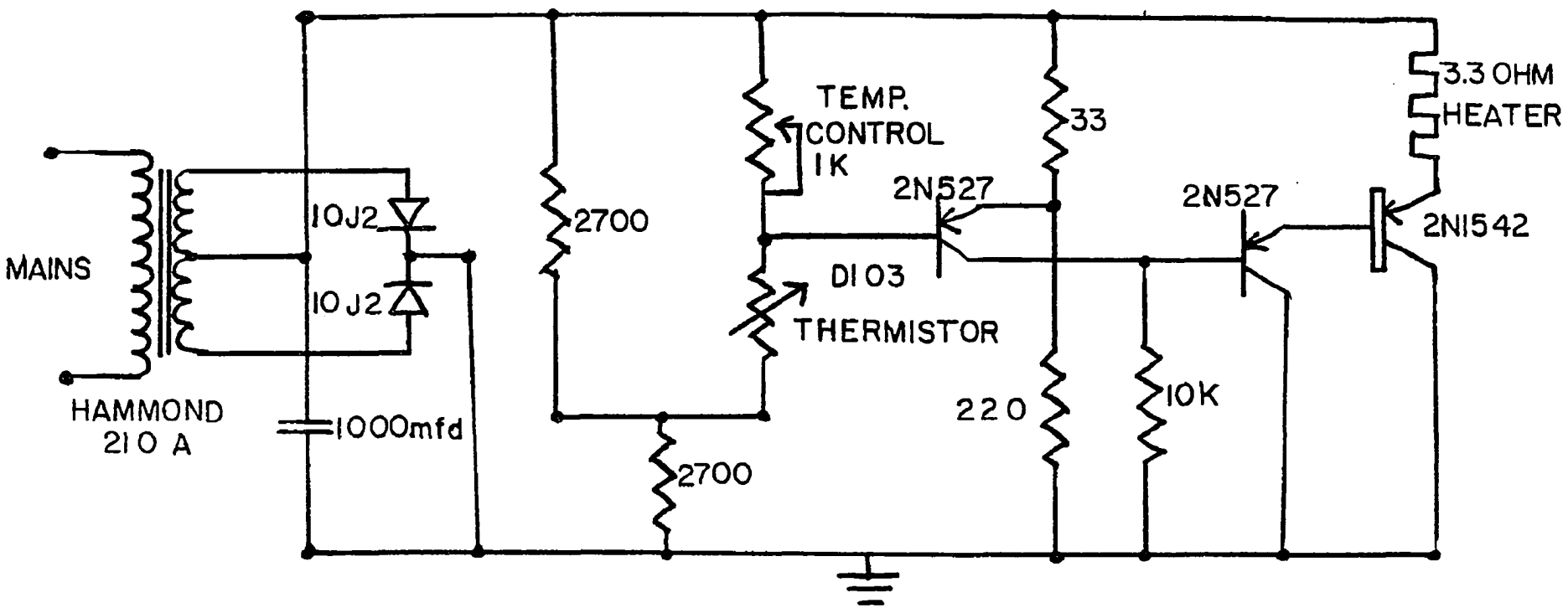

Figure (11) The Lamp Heater Controller Circuit

photograph the interference fringes. The camera and its auxiliary lens were mounted on an optical bench.

CHAPTER V

EXPERIMENTAL PROCEDURE

Determination of Intensities

The relative intensities of the spectral lines were measured with a Dumont 6911 multiplier phototube which has a type S-1 (Ag-O-Cs) photocathode surface with a peak sensitivity in the region 7000-9000 Å. The phototube was mounted in a light-tight metal case which was placed against the exit slit of the monchromator. The high voltage was supplied to the phototube by a Philips high voltage supply, Model PW 4024/01, which is specified as having an output variation of less than 0.005% for 1% mains voltage fluctuation. The output of the phototube was recorded by means of a Leeds and Northrup microampere strip chart recorder, which monitored continuously variations in lamp intensity. Each time the operating conditions of a lamp were changed, the intensity was allowed to come to equilibrium, which required a few minutes. The intensity of the Osram lamp was determined as a function of the lamp current. In the case of the Varian lamp no change in operating conditions was possible. The intensity of the new radiofrequency lamp was determined as a function of the temperature of the lamp base.

It may be seen from Equation (42) that, within a given order, cos θ or, near the centre of the interference pattern, θ, is directly proportional to the wavelength. Thus the distribution of intensity across a single fringe corresponds to the profile of the spectral line producing the fringe.

Since the resonance lines of potassium and rubidium lie at the limit of the visible spectrum, the interference fringes could not be observed visually. It was found convenient to use sodium yellow light from an Osram lamp in aligning the interferometer. In order that parallel light should be incident on the interferometer, an f/4.3 achromatic collimating lens of focal length 22 cm. was placed so that the exit slit of the monochromator was in its focal plane. With the interferometer placed correctly, so that the parallel beam was normal to the mirrors, the reflected light passed through the collimating lens and formed an image of the exit slit exactly coincident with the exit slit itself. Final adjustments of focus and mirror parallelism were made by placing a clear photographic plate in the plate holder of the camera, and observing with a magnifier the image of the fringes focussed on the grain of the photographic emulsion. When adjustment was complete, the system was covered to prevent stray light from entering the camera. Kodak Spectroscopic Plates, type 1N, with peak sensitivity in the range 7700-8400 Å, were used to photograph the fringes. Exposures were of five seconds duration, with compensation for varying source intensities being made by adjusting the variable apertures. In this way it was possible to obtain interference fringes of approximately equal peak intensities throughout the range of light sources. It should be noted that the intensity of an interference fringe at its peak is proportional to the peak intensity of the spectral line producing it, whereas the signal recorded

by a photomultiplier tube is proportional to the integrated intensity of the spectral line, when the monochromator slits are wide. The camera allowed for horizontal racking of the plates so that six exposures could be placed on each plate. The plates were developed in Kodak D-19 developer.

Since the response of the photographic emulsion is nonlinear it was necessary to carry out a calibration of the plates. The interferometer was removed from the parallel beam, so that only the monochromator exit slit was photographed. The flux density of light at the photographic plate was proportional to the area of the aperture in the parallel beam, which was varied so that a wide range of darkening was produced on the plate for a series of five-second exposures. This was repeated for each spectral line under investigation. The densities of the exposed plates were determined by scanning them with the Jarrell-Ash Model 2310 recording microphotometer. Calibration curves for the photographic emulsion were then obtained by plotting the recorder readings vs. the corresponding aperture areas.

Traces of the interference fringe patterns were obtained by scanning the plates with the microphotometer. Using the plate calibration curves the intensities were obtained at various points along the profiles of the interference fringes. These in turn yielded the intensity profiles of the corresponding spectral lines. The half-intensity points were determined for all the fringes, and, in the case of self-reversed spectral lines, the ratios of the intensities of the peaks to those of the central minima were also found. The half-widths of the spectral lines were obtained by measuring the diameters of the Fabry-Perot fringes as shown in Figure (12). This was done for up to five fringes on each exposure, and the squares of the diameters were written in the "rectangular array" given by Tolansky (1931). The half-widths were then calculated using Equation (51). This procedure was carried out for each spectral line over a range of operating conditions of the source.

Figure (12) gives the appearance of a microphotometer trace in which two fringes have been scanned.

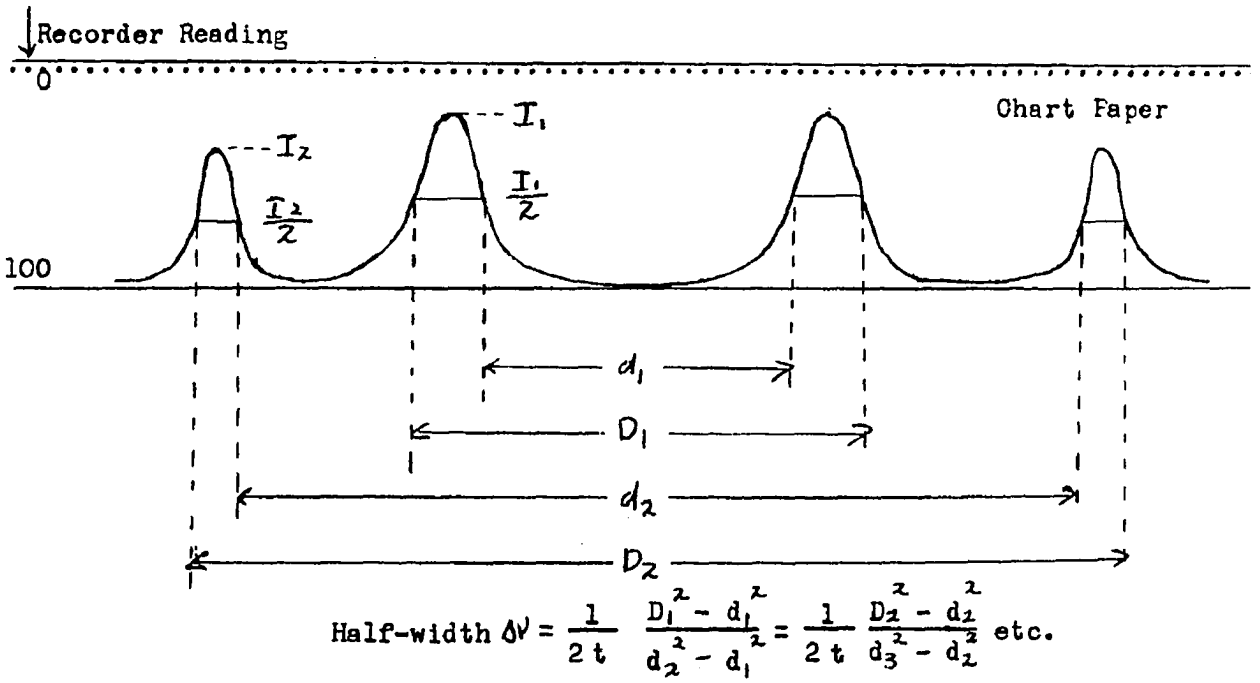

Figure (12) Measurements Made on Traces of the Interference Patterns in Determining Half-Widths.

The interferometer mirror spacings used in the experimental runs were the following:

Potassium Osram lamp: 1.93, 4.02, 4.88, and 7.26 mm.

Potassium radiofrequency lamp: 4.88, 7.00, 9.00, and 12.00 mm.

Rubidium Osram lamp: 1.00, 1.93, 3.04, and 5.68 mm.

Rubidium radiofrequency lamps: 3.04, 3.90, 4.92, and 5.68 mm.

The rubidium hyperfine structure separations were measured with mirror spacings of 10.03 and 12.00 mm.

CHAPTER VI

DISCUSSION OF THE RESULTS

The Potassium Lamps

(i) Integrated Intensities

The integrated intensities of the resonance spectral lines, as recorded by the photomultiplier tube, are given in Table (4), and are plotted in Figure (13), which shows variations in the integrated intensity as a function of lamp current in the case of the Osram lamp and as a function of temperature in the case of the radiofrequency lamp. The values for the two lamps are plotted simultaneously for purposes of comparison. The emission of the Osram lamp shows a slight minimum, which may be attributed to the rapid rise in self-absorption with rise in vapour pressure resulting from the increased current. The electrodeless discharge lamp produces more intense resonance lines than the Osram Lamp. As the vapour pressure is increased the combined intensity of the two lines shows a maximum at a temperature of 180°C., corresponding to a vapour pressure of 2.6×10^{-3} mm. Hg. The ratios of the intensities of the two components (7665Å : 7699Å) are not equal to the ratio of the statistical weights of the excited states, 2 : 1 ($^2P_{3/2}$: $^2P_{1/2}$). This indicates that at all times some self-absorption is taking place, since the absorption coefficient for the 7665Å component is twice as large as that for the 7699Å component.

(ii) Spectrum of the Radiofrequency Lamp

A brief investigation of the spectrum of the radiofrequency lamp was made, using the Hilger and Watts Model D 186 constant deviation wavelength spectrometer. Microphotometer traces of photographs of the

Table (4)

Relative Integrated Intensities of Resonance Lines
emitted by the Potassium Lamps
in Arbitrary Units

Osram Lamp			New Radiofrequency Lamp		
Operating Current Amps.	Intensity of 7665 Å Line	Intensity of 7699 Å Line	Operating Temp. °C.	Intensity of 7665 Å Line	Intensity of 7699 Å Line
0.6	42	25	70	65	58
0.7	50	40	80	74	62
0.8	52	43	90	76	63
0.9	57	46	100	77	64
1.0	59	47	110	79	65
1.1	59	47	120	82	69
1.2	58	46	130	83	72
1.3	58	45	140	85	77
1.4	57	44	150	86	79
1.5	56	42	160	89	80
1.6	56	41	170	90	80
1.7	59	43	180	92	80
1.8	62	46	190	92	78
1.9	66	49	200	93	75
2.0	73	53	210	93	75
			220	93	74
			230	93	74

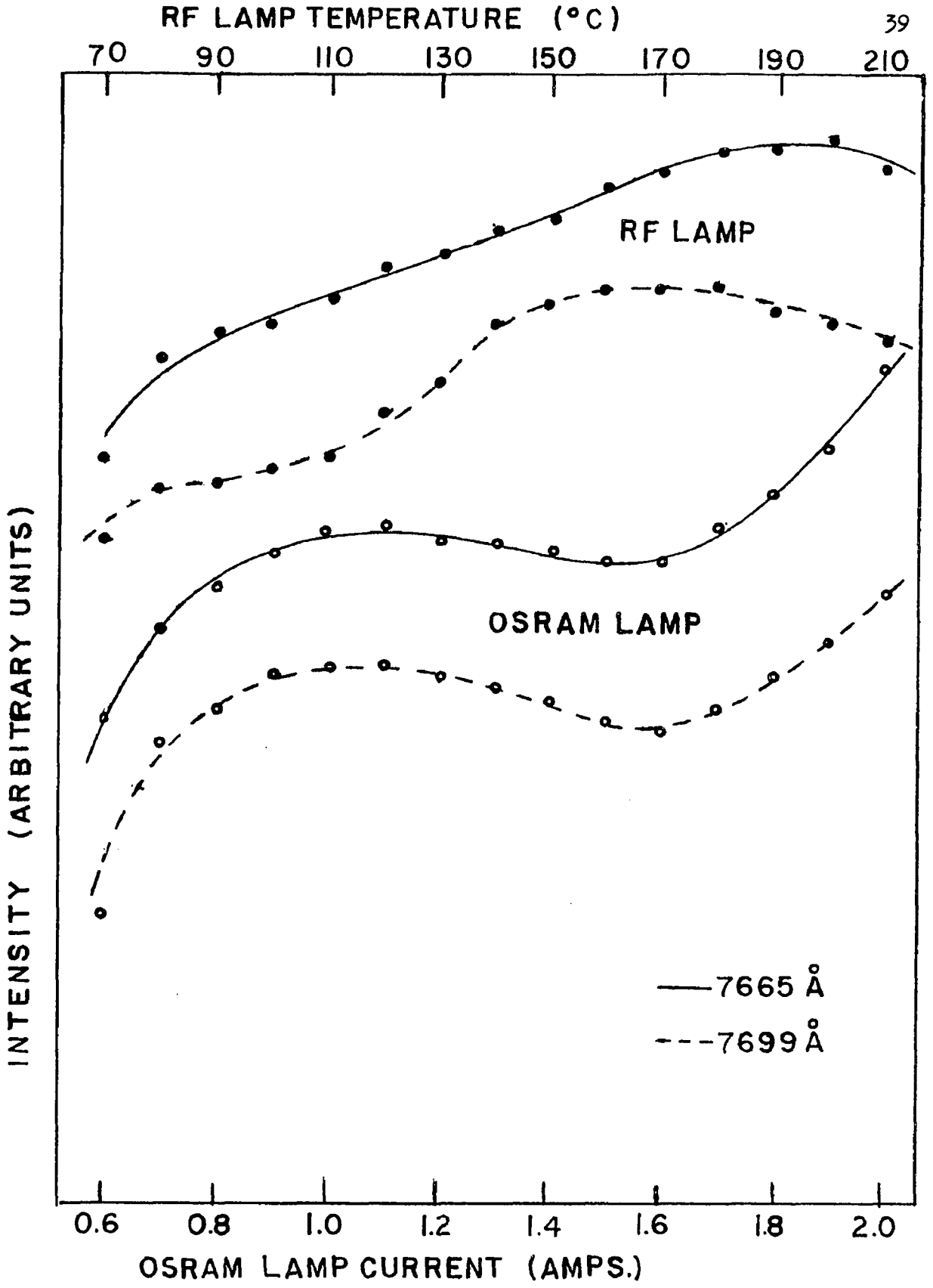

Figure (13) Integrated Intensities of the Osram and Radiofrequency Potassium Lamps as functions of the Operating Parameters

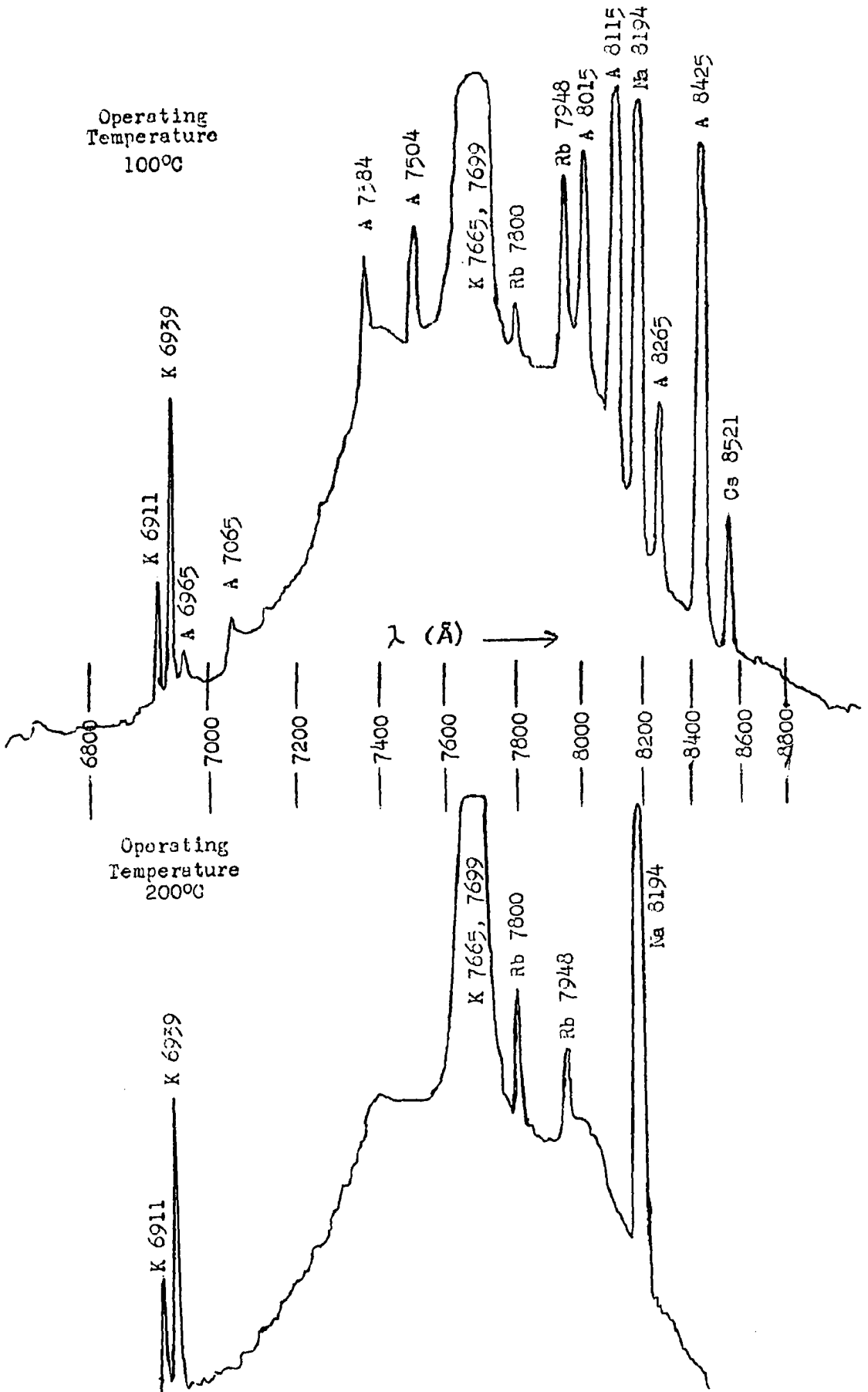

Figure (14) Spectrum in the Range 6500 - 8500 Å Emitted by the Radiofrequency Potassium Lamp.

spectrum in the range 6500 - 8500 Å are shown in Figure (14) for lamp temperatures of 100°C and 200°C. These show spectral lines emitted by the other alkali metals, which are present as impurities. It is also shown that the intensity of the argon emission is reduced as the potassium vapour pressure is increased.

(iii) Half-widths of the Resonance Lines

The average values of the half-widths were obtained from the diameters of the Fabry-Perot fringes as outlined in Chapter V. Photographs of typical fringe systems and the corresponding microphotometer traces are shown in Figures (15) and (16). The numerical values of the half-widths are given in Tables (5) and (6) and are plotted in Figures (17) and (18) as functions of the operating parameters of the lamps. Also plotted are the separations of the self-reversal maxima, which increase in the same manner as the half-widths. The half-width of the 7665 Å component emitted by the Osram lamp varies from 0.27 $cm.^{-1}$ to 1.1 $cm.^{-1}$ in the range 0.6-1.7 amperes, and is approximately proportional to the operating current. The corresponding variation for the 7699 Å component over the same range extends from 0.21 $cm.^{-1}$ to 0.74 $cm.^{-1}$. The half-widths of the lines emitted by the new radiofrequency lamp are much smaller and increase nearly linearly with temperature over the entire temperature range of 70°C to 210°C. The half-width of the 7665 Å line varies from 0.097 $cm.^{-1}$ to 0.26 $cm.^{-1}$, while that of the 7699 Å line varies from 0.095 $cm.^{-1}$ to 0.21 $cm.^{-1}$.

(iv) Peak Intensities

The ratios of the peak intensities of the corresponding resonance lines produced by the various lamps under normal operating conditions were

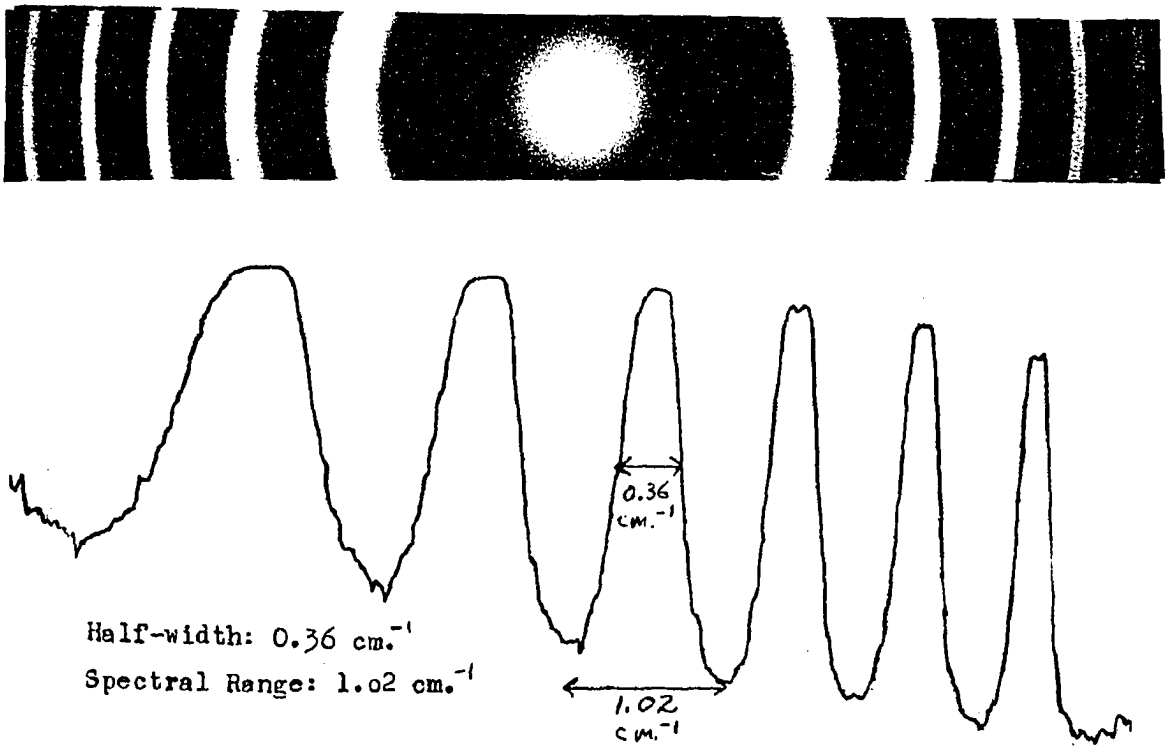

Figure (15a) Photograph of Fringe System and Microphotometer Trace (one-half of fringe system) for Osram lamp at 0.9 ampere, 7665 Å line.

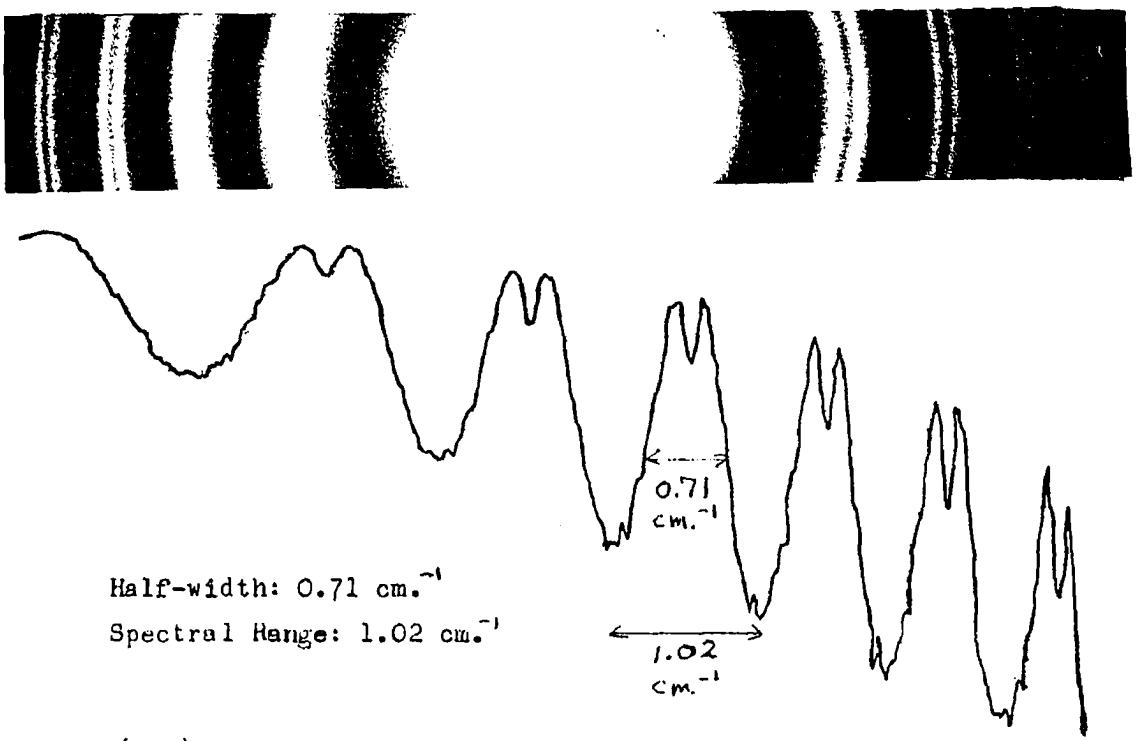

Figure (15b) Photograph of Fringe System and Microphotometer Trace for Osram lamp at 1.5 amperes, 7665 Å line.

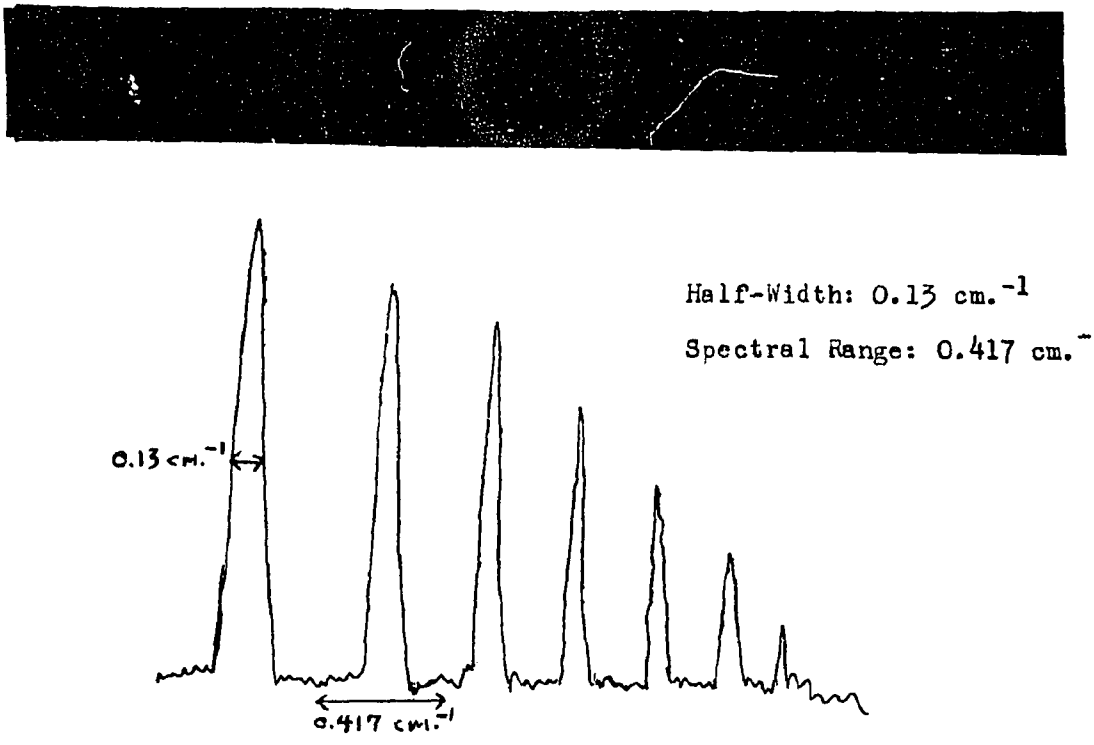

Figure (16a) Photograph of Fringe System and Microphotometer Trace for the 7665 Å Line Emitted by the Radiofrequency Lamp, Operating at 120°C.

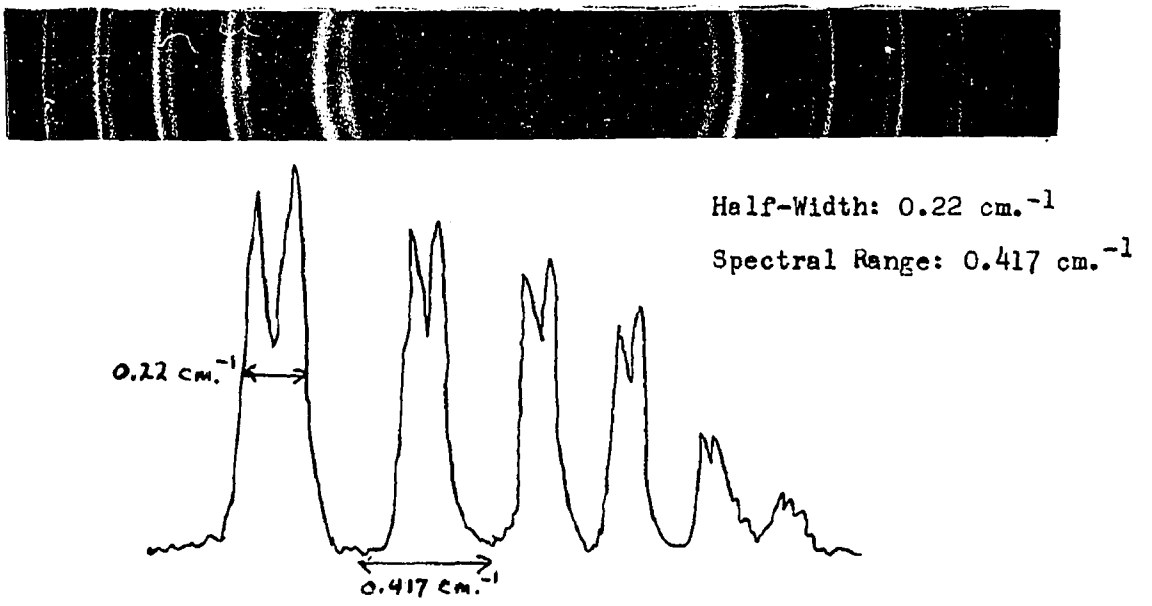

Figure (16b) Photograph of Fringe System and Microphotometer Trace for the 7665 Å Line Emitted by the Radiofrequency Lamp, Operating at 170°C.

Table (5)

Half-Widths, and Separations of the Self-Reversal Maxima in the Potassium 7665Å Component

Osram Lamp			New Radiofrequency Lamp		
Operating Current Amps.	Half-Width $cm.^{-1}$	Separ. of Maxima $cm.^{-1}$	Operating Temp. $^{o}C.$	Half-Width $cm.^{-1}$	Separ. of Maxima $cm.^{-1}$
0.6	0.270		70	0.0968	
0.7	0.299		80	0.105	
0.8	0.337	0.0657	90	0.110	
0.9	0.358	0.0837	100	0.126	0.0347
1.0	0.396	0.0874	110	0.131	0.0556
1.1	0.472	0.120	120	0.150	0.0716
1.2	0.509	0.167	130	0.175	0.0828
1.3	0.554	0.220	140	0.182	0.0881
1.4	0.633	0.248	150	0.190	0.0937
1.5	0.714	0.271	160	0.211	0.103
1.6	0.871	0.327	170	0.219	0.108
1.7	1.05	0.430	180	0.231	0.111
1.8	1.47	0.542	190	0.242	0.117
1.9	1.61	0.648	200	0.252	0.119
2.0	1.66	0.726	210	0.260	0.123

Table (6)

Half-Widths, and Separations of the Self-Reversal Maxima in the Potassium 7699Å Component

Osram Lamp			New Radiofrequency Lamp		
Operating Current Amps.	Half-Width cm.$^{-1}$	Separ. of Maxima cm.$^{-1}$	Operating Temp. °C.	Half-Width cm.$^{-1}$	Separ. of Maxima cm.$^{-1}$
0.6	0.213		70	0.0953	
0.7	0.199		80	0.0988	
0.8	0.227		90	0.104	
0.9	0.240		100	0.114	
1.0	0.288	0.0576	110	0.125	
1.1	0.317	0.0703	120	0.130	
1.2	0.340	0.0781	130	0.145	0.0514
1.3	0.409	0.0922	140	0.153	0.0600
1.4	0.460	0.138	150	0.161	0.0612
1.5	0.480	0.176	160	0.178	0.0652
1.6	0.628	0.221	170	0.187	0.0686
1.7	0.739	0.264	180	0.190	0.0733
1.8	1.03	0.329	190	0.199	0.0737
1.9	1.12	0.406	200	0.203	0.0739
2.0	1.47	0.503	210	0.207	0.0751

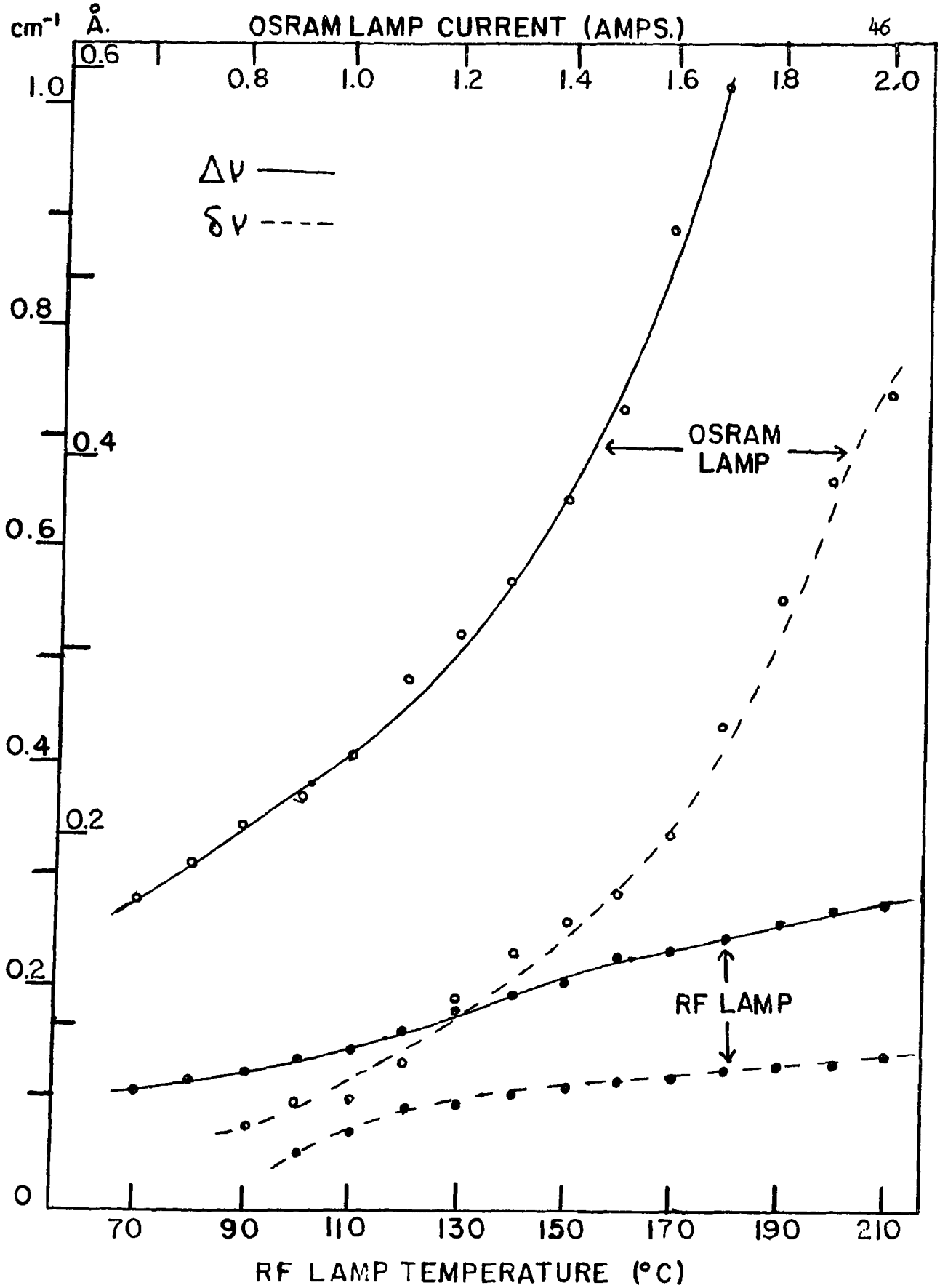

Figure (17) Half-Widths, $\Delta\nu$, and Separations of the Self-Reversal Maxima, $\delta\nu$, in the Potassium 7665 Å Component.

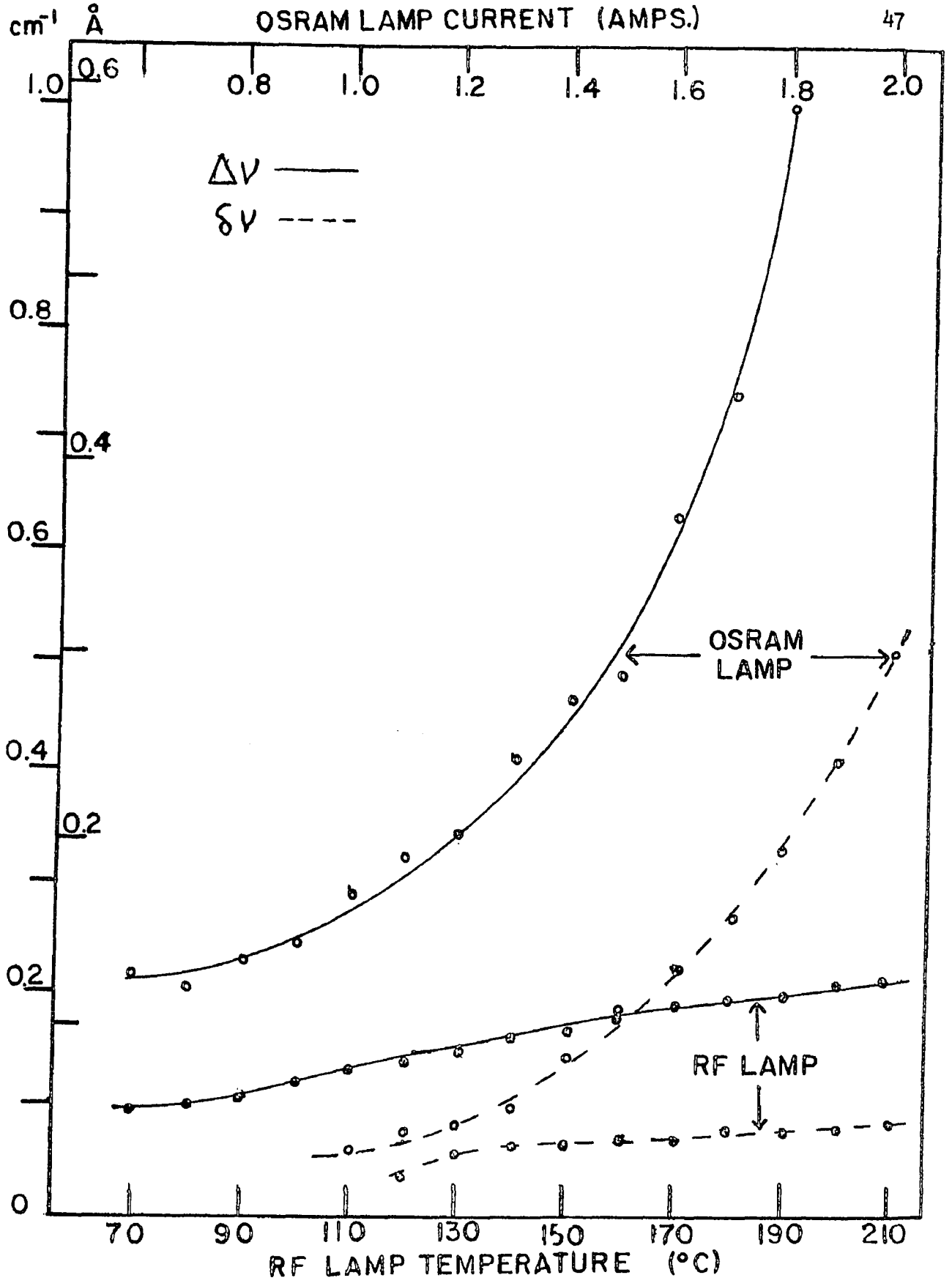

Figure (18) Half-Widths, $\Delta\nu$, and Separations of the Self-Reversal Maxima, $\delta\nu$, in the Potassium 7699 Å Component.

determined approximately, since they are the reciprocals of the ratios of the amounts of light allowed to enter the camera when photographing the interference fringes. Using this method, the ratio of the peak of a line produced by the radiofrequency potassium lamp to that emitted by the Osram lamp is approximately 3.6 : 1. The ratio of the integrated intensities is approximately 1.6 : 1. Assuming a rectangular line shape for the sake of simplicity, the integrated intensity is the product of the line width and its peak intensity. On this basis, the ratio of the line widths produced by the radiofrequency and the Osram lamps should be $\frac{1.6}{3.6} : 1 = 1 : 2.3$. When the radiofrequency lamp is operated at a temperature of 130°C and the Osram lamp is operated at a current of around one ampere, the ratio of the line widths has an average value of 1 : 2.1. Under these operating conditions the lines are strongly absorbed and so are flat-topped and nearly rectangular in shape. If the Osram lamp is operated in the range 1.0 - 1.6 amperes the widths of the lines increase rapidly, but there is no corresponding increase in the integrated intensity because the effect of the self-reversal is to decrease the intensity at the centre of the line. These approximate spectral line shapes are shown in Figure (25).

(v) Self-Reversal

Values of $\frac{I_{max}}{I(\nu_0)}$ and of the absorption parameter, p, defined in Chapter II, are given in Tables (7) and (8), and values of $\frac{I_{max}}{I(\nu_0)}$ are plotted in Figures (19) and (20) for the resonance lines of potassium produced by the Osram lamp and the radiofrequency lamp respectively. Self-reversal appears in the lines emitted by the Osram lamp when the operating current is greater than one ampere, and, in the case of the radiofrequency lamp, when the operating temperature is greater than 120°C. It was observed

Table (7)

Values of the Ratios of Intensities of Self-Reversal Peaks to Central Minima, $\frac{I_{max}}{I(\nu_c)}$, and of the Absorption Parameter p.

Osram Potassium Lamp

Operating Current Amps.	7665 Å Line		7699 Å Line	
	$\frac{I_{max}}{I(\nu_c)}$	p	$\frac{I_{max}}{I(\nu_c)}$	p
0.8	1.03	1.26		non-self-reversed
0.9	1.07	1.40		
1.0	1.08	1.44	1.05	1.33
1.1	1.08	1.44	1.05	1.33
1.2	1.12	1.55	1.07	1.40
1.3	1.17	1.66	1.08	1.44
1.4	1.25	1.82	1.11	1.52
1.5	1.28	1.88	1.13	1.57
1.6	1.33	1.96	1.19	1.71
1.7	1.40	2.06	1.25	1.82
1.8	1.51	2.20	1.47	2.15
1.9	1.57	2.28	1.57	2.28
2.0	1.55	2.25	1.54	2.22

Table (8)

Values of the Ratios of Intensities of Self-Reversal Peaks to Central Minima, $\frac{I_{max}}{I(\nu_0)}$, and of the Absorption Parameter p.

Radiofrequency Potassium Lamp

Operating Temp. °C	7665 Å Line		7699 Å Line	
	$\frac{I_{max}}{I(\nu_0)}$	p	$\frac{I_{max}}{I(\nu_0)}$	p
100	1.06	1.36	non-self-reversed	
110	1.08	1.44		
120	1.10	1.50	1.03	1.26
130	1.17	1.66	1.08	1.44
140	1.25	1.82	1.13	1.57
150	1.30	1.91	1.16	1.64
160	1.40	2.06	1.21	1.75
170	1.50	2.23	1.24	1.81
180	1.56	2.26	1.28	1.88
190	1.66	2.38	1.30	1.91
200	1.77	2.50	1.33	1.96
210	1.80	2.52	1.38	2.03

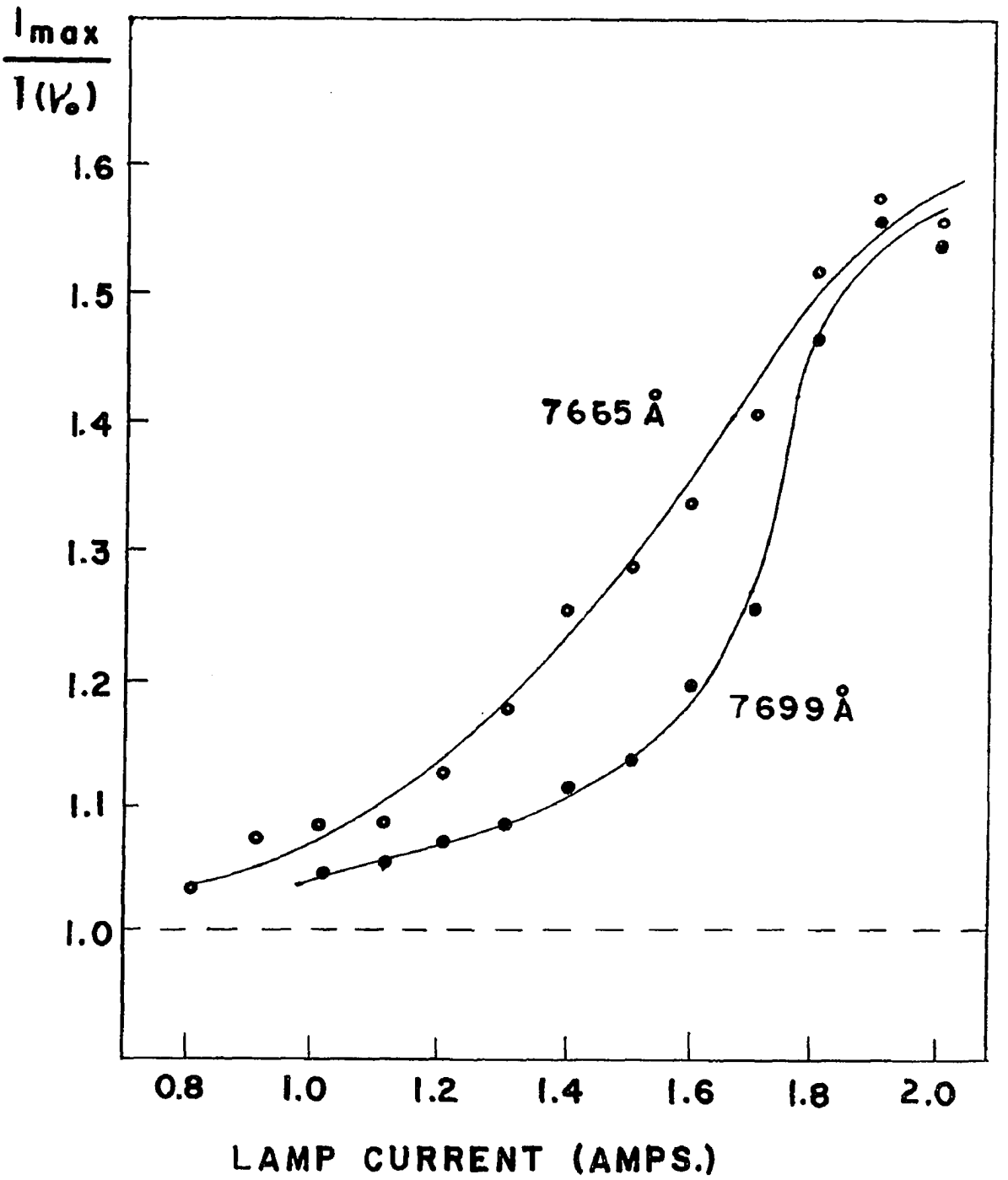

Figure (19) Ratios of Intensities of Self-Reversal Peaks to Central Minima; Osram Potassium Lamp.

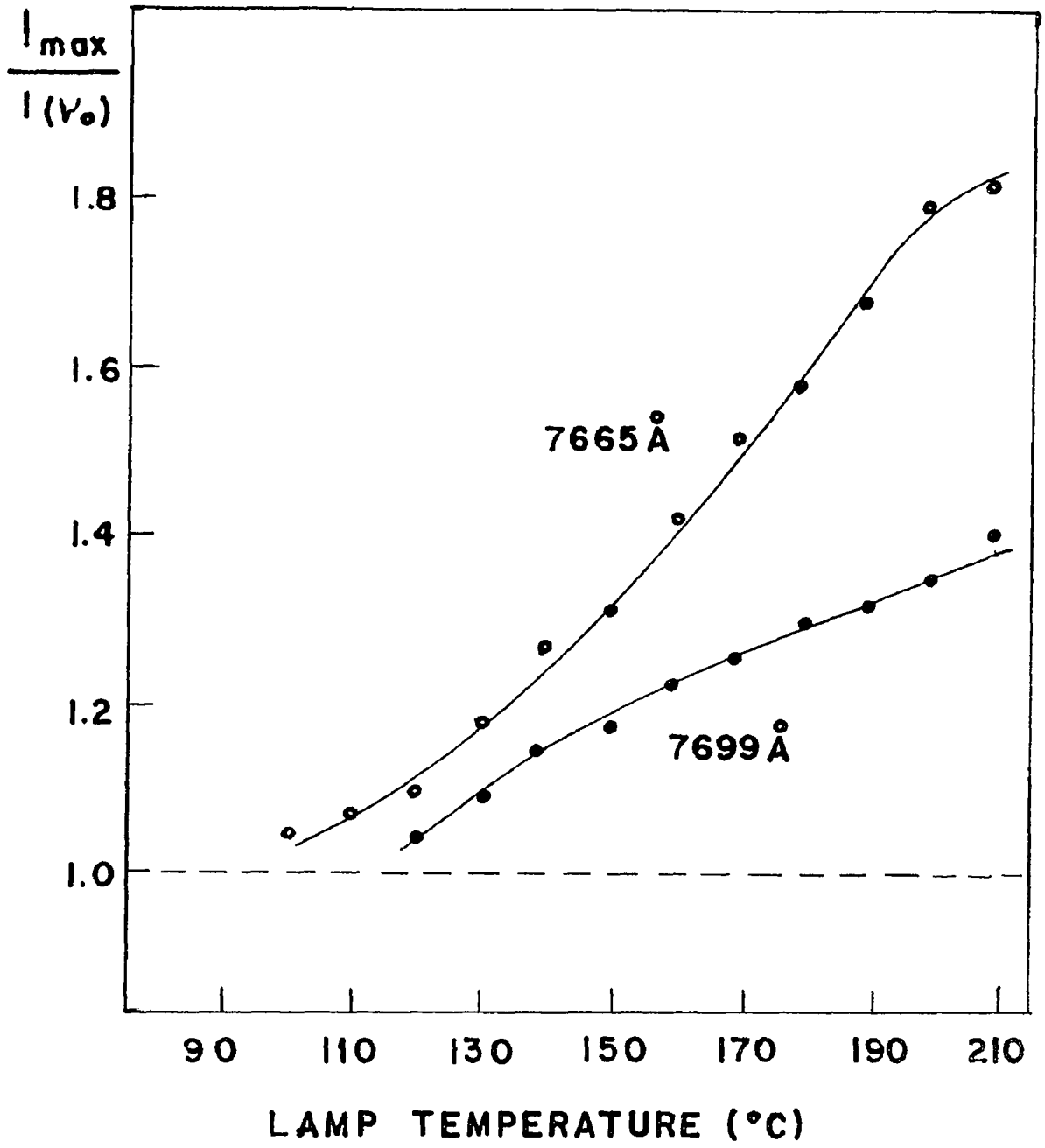

Figure (20) Ratios of Intensities of Self-Reversal Peaks to Central Minima; Radiofrequency Potassium Lamp.

by Chapman (1964) that the effectiveness of the radiofrequency potassium lamp in exciting resonance fluorescence decreased when the lamp was operated at temperatures above 120°C, which demonstrates the necessity of employing non-self-reversed resonance lines as the exciting radiation. However, due to their initial higher intensities, heavily self-reversed lines obtained from the radiofrequency source retain greater intensities at their centres than those obtained from the Osram lamp.

Self-reversal occurs in the Osram lamp because the ionic discharge and thus the excitation are concentrated about the central axis of the discharge tube, whereas the reverse of this distribution occurs in the radiofrequency-excited discharge. The skin effect tends to concentrate the radiofrequency field and the excitation in a thin layer near the walls of the discharge tube; viewed end-on, the emission is in the form of a ring. This effect becomes more pronounced at higher vapour pressures. Under these conditions the light emitted at the back wall of the discharge tube would be greatly absorbed in passing through the central region of low excitation. In addition, there may be absorption near the walls due to the presence of a layer of cooler vapour, since the discharge tube was exposed, and of a higher density of unexcited atoms as a result of de-excitation by collisions with the walls.

(vi) Emission from Different Sections of the Radiofrequency Discharge Tube

A brief investigation was made of the line profiles emitted by the central region and by a section near the edge of the discharge tube. This was accomplished by placing a slit of width 2 mm. at a distance of about 8 cm. from the monochromator entrance slit. The lamp was placed near the auxiliary slit so that only the light emitted from a vertical section through the discharge tube passed through both slits and entered

the monochromator. The half-widths, separation of self-reversal peaks, and ratios of self-reversal peaks to minima were not significantly different from those obtained previously. It was found that the half-widths, separations of self-reversal maxima, and ratios of peak intensity to the central minima were greater for light emerging from the edge by factors of 1.20, 1.54, and 1.09, respectively, in the case of 7665 Å radiation. The corresponding factors for the 7699 Å line were 1.11, 1.30, and 1.04. These results indicate that there was self-absorption occuring in a layer of vapour near the walls, since the light emitted tangentially, without passing through the central region, was still subject to absorption.

The Rubidium Lamps

(i) Integrated Intensities

The integrated intensities of the resonance lines are given in Table (9) and plotted in Figure (21) similarly to those of the potassium lamps. In the case of the Osram lamp the intensity shows a minimum at a lower value of the lamp current than with the potassium Osram lamp. The resonance lines emitted by the radiofrequency lamp are several times more intense under ordinary operating conditions. The combined intensity of the two resonance lines shows a maximum at a temperature of 150°C, corresponding to a vapour pressure of 1.2×10^{-3} mm. Hg, which is of the same order of magnitude as in the case of potassium. The intensity peak is more pronounced in the case of rubidium, indicating a greater effect of vapour pressure on the conditions of the discharge. The rubidium intensities decrease very rapidly below the temperature of 110°C; that is, for vapour pressure less than 3.7×10^{-4} mm. Hg. Bell, Bloom, and Lynch (1961) attribute this behaviour to a competition between argon and rubidium discharges with the result that, near this critical vapour pressure, the emission is predominantly due to either argon or rubidium atoms.

(ii) Half-Widths of the Resonance Lines

The half-widths and, in the case of the Osram lamp, the separation of the self-reversal peaks, were obtained from the Fabry-Perot patterns. Photographs and the corresponding microphotometer traces of typical fringe patterns are shown in Figure (22). Numerical values are given in Tables (10) and (11) and are plotted in Figures (23) and (24). The half-width of the 7800 Å line emitted by the Osram lamp varies from 0.51 $cm.^{-1}$ to 3.0 $cm.^{-1}$ in the range 0.6 to 1.5 amperes. The rate of increase of

Table (9)

Relative Integrated Intensities of Resonance Lines emitted by the Rubidium Lamps.

Arbitrary Units

Osram Lamp			New Radiofrequency Lamp		
Operating Current Amps.	Intensity of 7800 Å Line	Intensity of 7948 Å Line	Operating Temp. °C.	Intensity of 7800 Å Line	Intensity of 7948 Å Line
0.6	17	13	70	7	6
0.7	15	11	80	7	6
0.8	13	10	90	9	7
0.9	12	8	100	12	9
1.0	12	8	110	78	69
1.1	14	10	120	77	70
1.2	18	12	130	77	71
1.3	24	16	140	75	71
1.4	33	21	150	72	69
1.5	39	25	160	69	65
1.6	44	28	170	66	62
1.7	48	31	180	64	59
1.8	53	34	190	61	55
1.9	57	38	200	58	50
2.0	58	42	210	57	48

Varian Lamp

7800 Å Line: 70
7948 Å Line: 40

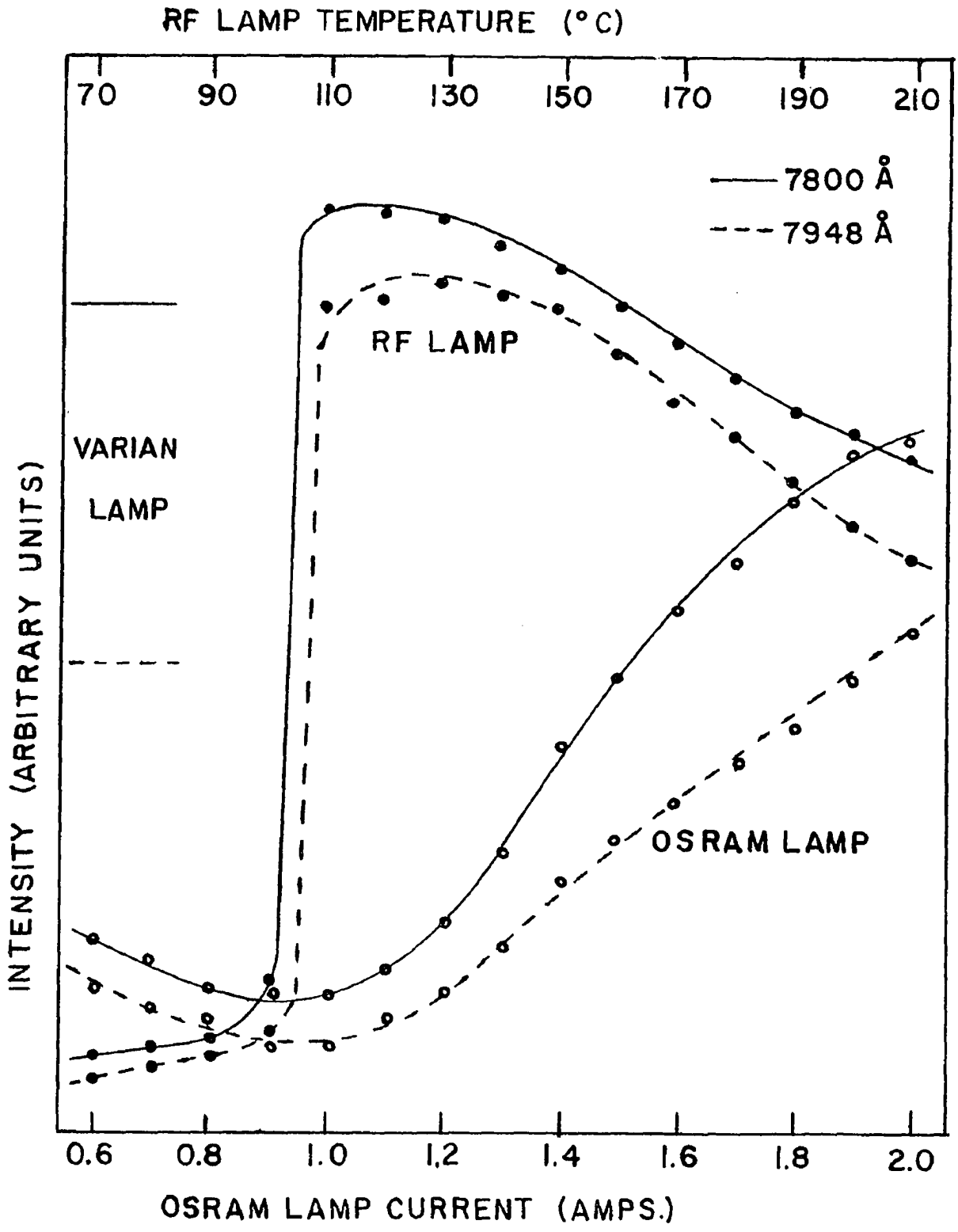

Figure (21) Integrated Intensities, in Arbitrary Units, of the Resonance Lines Emitted by the Rubidium Lamps.

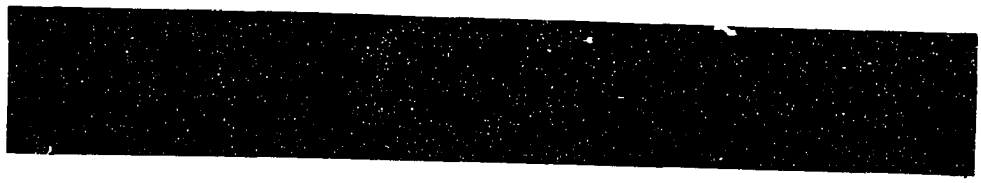

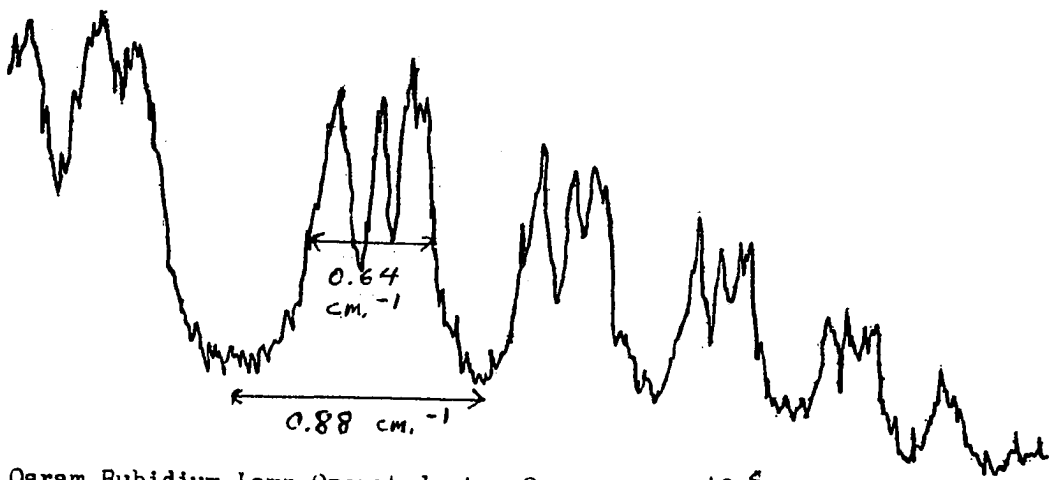

Osram Rubidium Lamp Operated at o.9 ampere, 7948 Å Component.

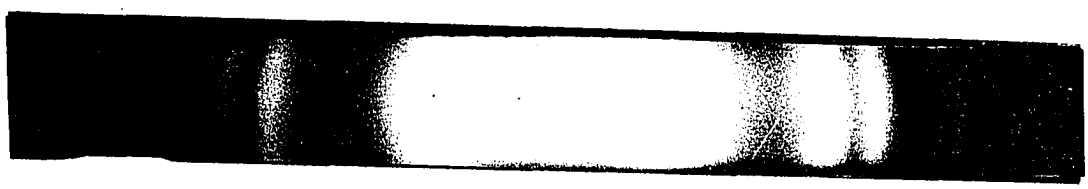

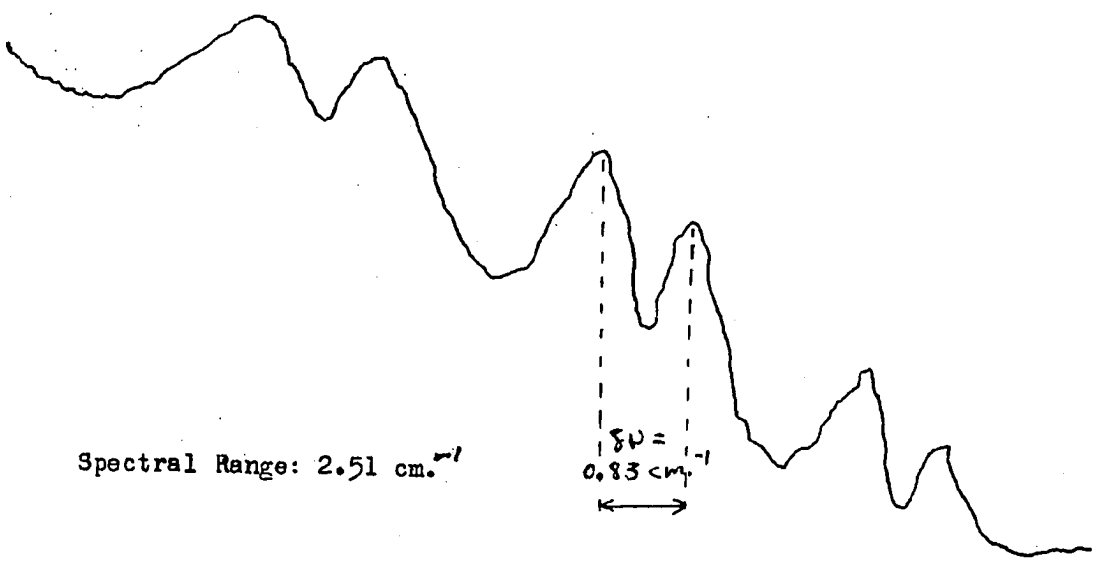

Osram Rubidium Lamp Operated at 1.3 amperes, 7800 Å Component.

Figure (22) Photographs of Fringe Patterns and Microphotometer Traces for the Resonance Lines Emitted by the Osram Rubidium Lamp.

Table (10)

Half-Widths, and Separations of the Self-Reversal Maxima in the Rubidium 7800Å Component

Osram Lamp			New Radiofrequency Lamp	
Operating Current Amps.	Half-Width cm.$^{-1}$	Separ. of Maxima cm.$^{-1}$	Operating Temp. °C.	Half-Width cm.$^{-1}$
0.6	0.508	non-	100	0.365
0.7	0.605	self-	110	0.387
0.8	0.672	reversed.	120	0.382
0.9	0.779		130	0.338
1.0	0.959	0.407	140	0.379
1.1	1.17	0.519	150	0.379
1.2	1.63	0.644	160	0.365
1.3	2.13	0.833	170	0.382
1.4	2.71	0.989	180	0.385
1.5	2.99	1.04	190	0.407
1.6	3.18	1.06	200	0.394
1.7	3.50	1.22	210	0.450
Varian Lamp Half-Width: 0.265 cm.$^{-1}$				

The radiofrequency lamps do not produce self-reversed lines.

Table (11)

Half-Widths, and Separations of the Self-Reversal Maxima in the Rubidium 7948Å Component

Osram Lamp			New Radiofrequency Lamp	
Operating Current Amps.	Half-Width cm.$^{-1}$	Separ. of Maxima cm.$^{-1}$	Operating Temp. °C.	Half-Width cm.$^{-1}$
0.6	0.457	non-	100	0.348
0.7	0.488		110	0.361
0.8	0.543	self-	120	0.366
0.9	0.644	reversed	130	0.315
1.0	0.717		140	0.371
1.1	0.864	0.405	150	0.367
1.2	1.22	0.438	160	0.375
1.3	1.48	0.608	170	0.393
1.4	1.60	0.722	180	0.400
1.5	1.95	0.973	190	0.384
1.6	2.40	1.11	200	0.408
1.7	2.88	1.15	210	0.451
Varian Lamp				
Half-Width: 0.265 cm.$^{-1}$				

The radiofrequency lamps do not produce self-reversed lines.

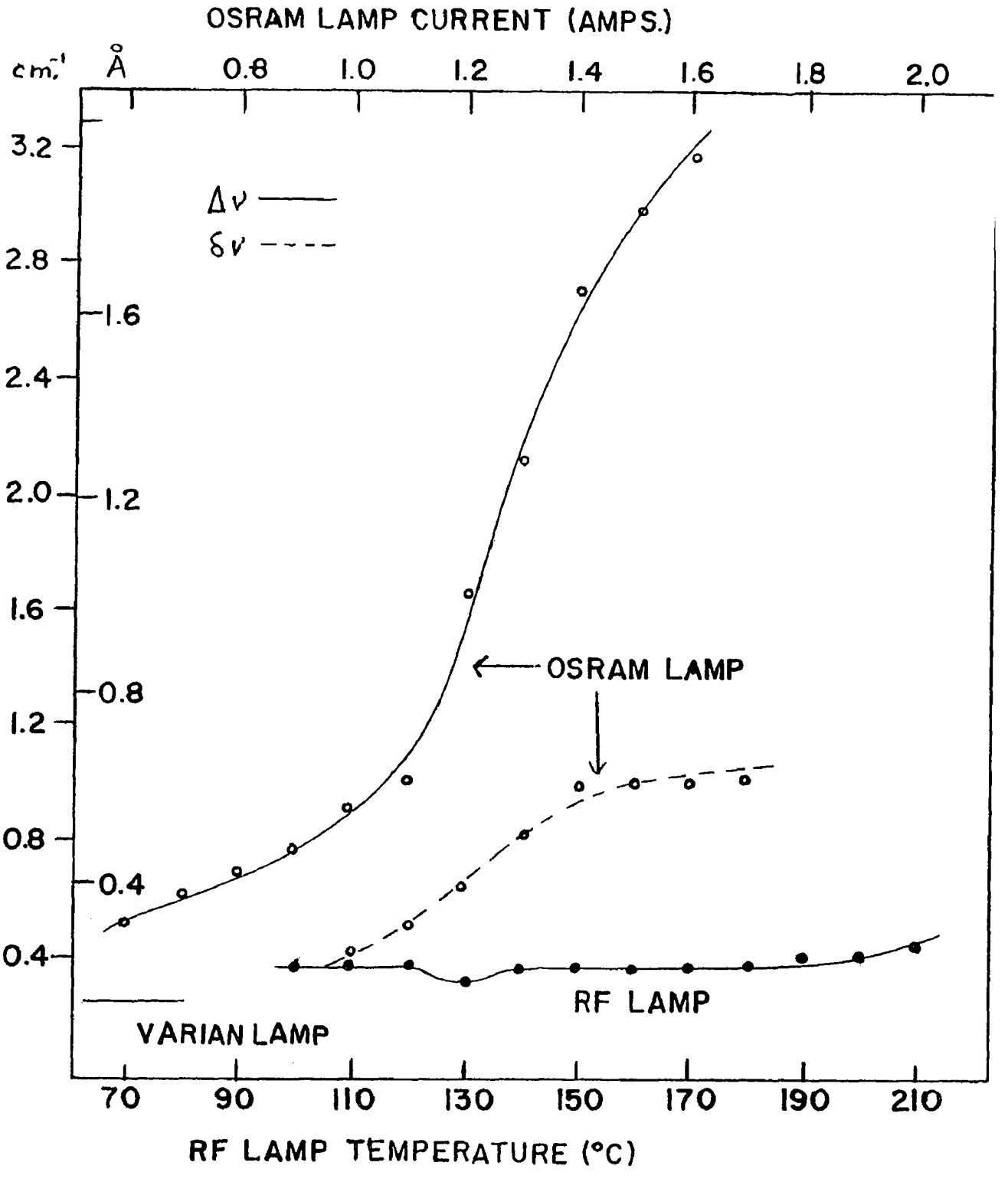

Figure (23) Half-Widths, $\Delta\nu$, and Separations of Self-Reversal Maxima, $\delta\nu$, for the Rubidium 7800 Å Component.

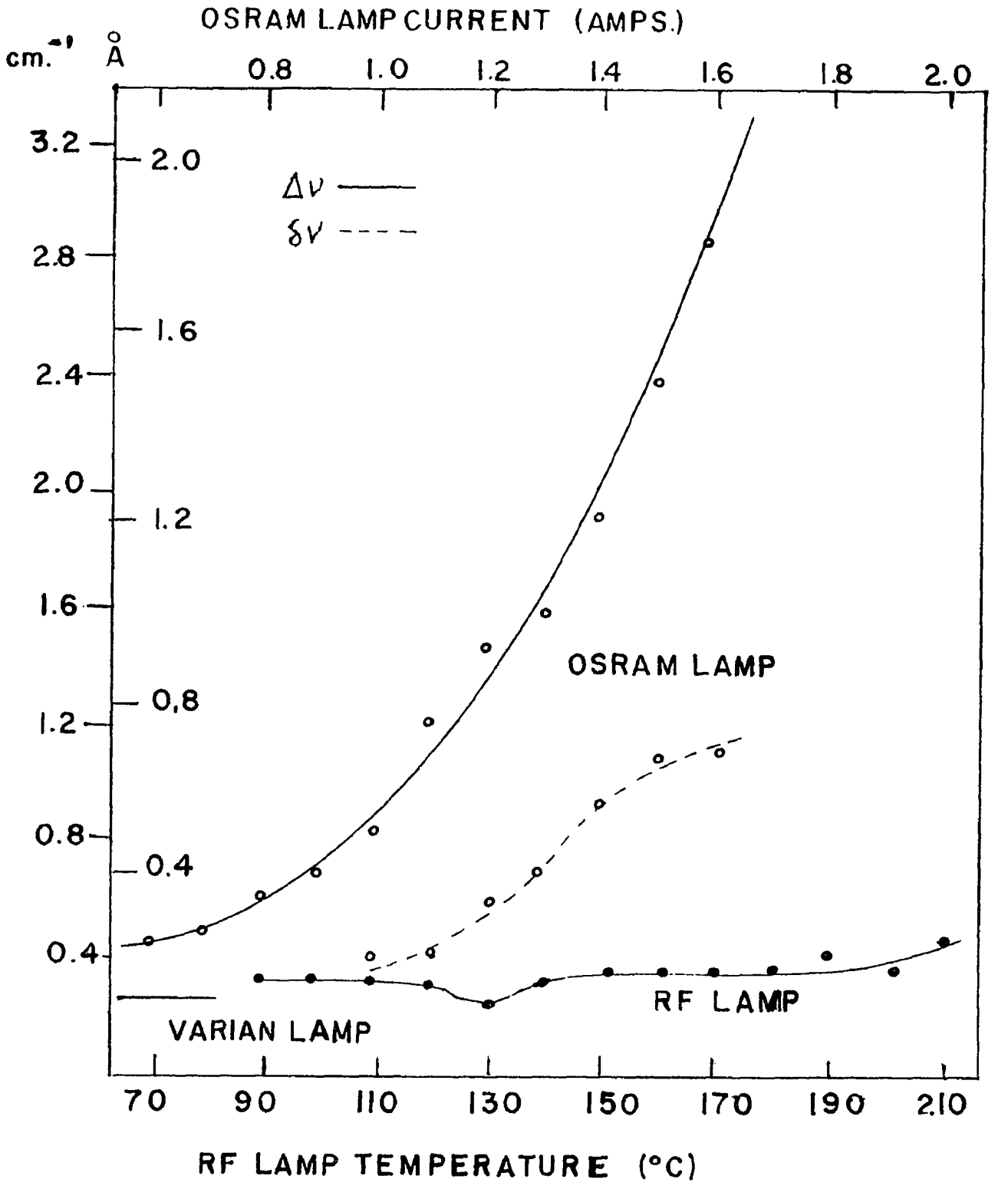

Figure (24) Half-Widths, $\Delta\nu$, and Separations of Self-Reversal Maxima, $\delta\nu$, for the Rubidium 7948 Å Component.

the half-width is greater for operating currents exceeding 1.1 amperes, which is also the region of rapid increase in integrated intensity. The corresponding variation for the 7948 Å component is 0.46 $cm.^{-1}$ to 2.0 $cm.^{-1}$. The half-widths of the lines emitted by the new radiofrequency lamp are very much smaller, and are less than 0.40 $cm.^{-1}$ for both components when the operating temperature is less than 200°C, corresponding to a vapour pressure of 3.80×10^{-2} mm. Hg. Above this temperature a definite increase in half-width occurs, and it may be seen from the data given in Table (2) that this increase is a result of self-pressure broadening. It should also be noted that a decrease in the half-widths of approximately 15% occurred consistently at a temperature of 130°C, which is the condition for maximum integrated intensity. The half-widths of the resonance lines emitted by the Varian rubidium lamp were found to be less than 0.30 $cm.^{-1}$. This small half-width may be due to the use of a krypton carrier gas, which provides an intense and stable discharge at the low operating temperature of 90°C. In addition, the hyperfine structure components of rubidium 87, which are at the extreme edges of the spectral lines, appear to be less intense in the lines emitted by the Varian lamp, indicating a difference in the relative abundances of the rubidium isotopes in the lamps. However, the hyperfine structure components are not sufficiently resolved to determine accurately their intensity ratios.

(iii) Peak Intensities

Calculations connecting peak intensities, integrated intensities, and half-widths have been carried out. The ratios of the peak intensities were determined from the ratios of the sizes of the apertures in the light beam when photographing the fringes. The densities of the photographed fringes indicate that the peak intensities of the lines emitted by the

new radiofrequency lamp are greater by a factor of 8 than those of the Osram lamp operated at 1.5 amperes. The corresponding integrated intensities are in the ratio 2 : 1. Assuming a rectangular line shape, the ratio of the widths is 1 : 4. However, in this case, the peak intensity of the lines emitted by the Osram lamp denotes the intensity of the self-reversal peaks. The reduction of intensity in the centre of the line is compensated for by a greater width; the experimental values of the half-widths are in the ratio 1 : 6.5, using the average half-width of the lines produced by the Osram lamp with an operating current of 1.5 ampere. The shapes of these lines and the corresponding shapes of the potassium lines emitted by the radiofrequency and Osram lamps are shown in Figure (25).

(iv) Self-Reversal

The ratios of the self-reversal peak intensities to those of the central minima are given in Table (12) and plotted in Figure (26) for the rubidium resonance lines obtained from the Osram lamp. Self-reversal appears when the lamp current is increased to 1.0 ampere, and the degree of self-reversal increases rapidly with current; with an operating current of 1.4 amperes the central minima have only 2/3 the intensity of the side maxima. The resonance lines emitted by the new radiofrequency lamp did not exhibit complete self-reversal, but each hyperfine structure component showed slight self-reversal when the lamp was operated at higher temperatures. The microphotometer traces in Figure (27) show self-reversal in some of the components. The Varian lamp emits hyperfine components with sharp central peaks because of its low operating temperature.

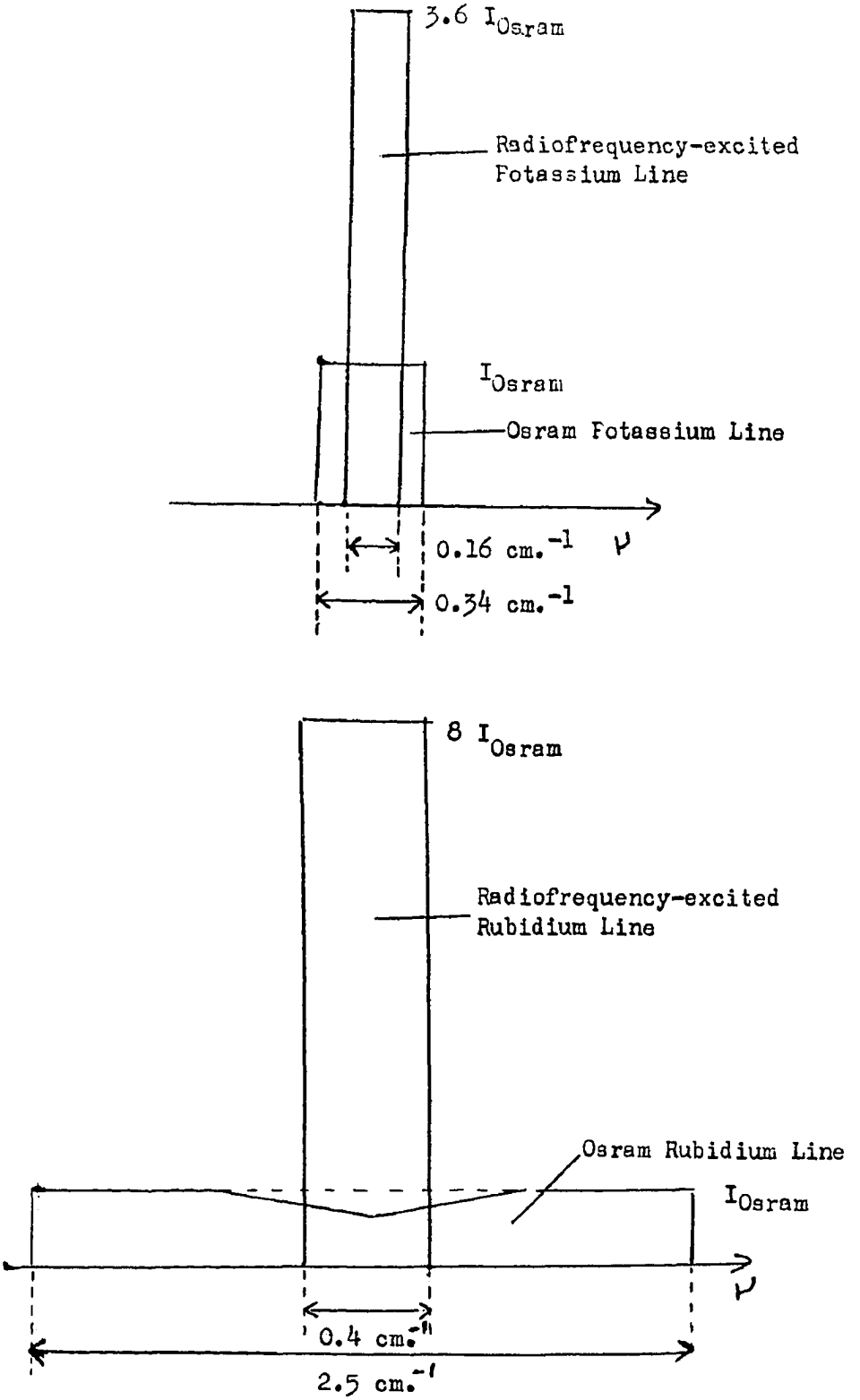

Figure (25) Approximate Shapes of the Potassium and Rubidium Spectral Lines Produced under Typical Operating Conditions.

Table (12)

Ratios of Intensities of Self-Reversal Peaks to Central Minima

Osram Rubidium Lamp

Operating Current Amps.	$\frac{I_{max}}{I(\nu_0)}$ 7800 Å Line	$\frac{I_{max}}{I(\nu_0)}$ 7948 Å Line
1.0	1.14	
1.1	1.22	1.17
1.2	1.31	1.29
1.3	1.45	1.38
1.4	1.58	1.53
1.5	1.65	1.55
1.6	1.68	1.89
1.7	1.75	1.63

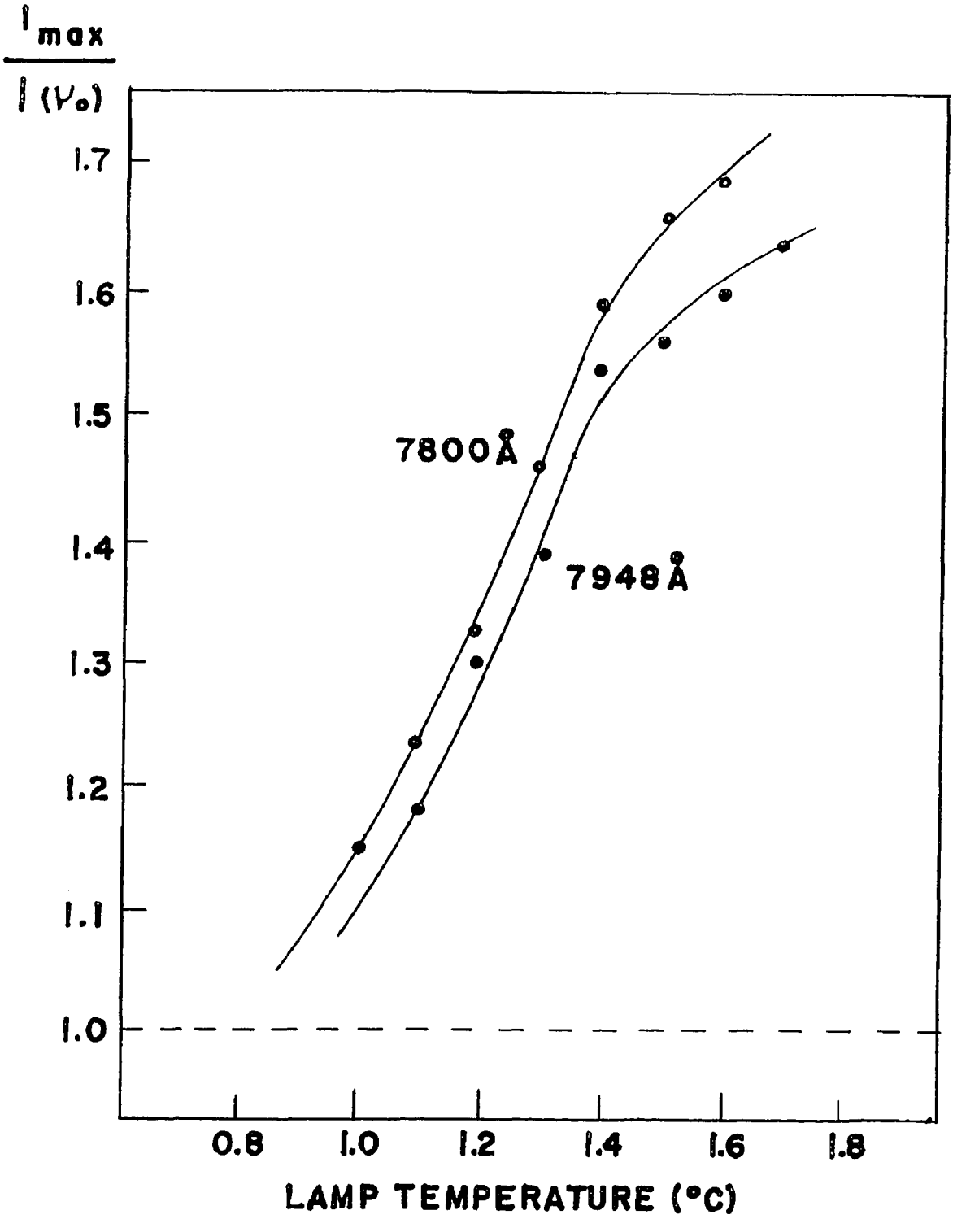

Figure (26) Ratios of Intensities of Self-Reversal Peaks to Central Minima; Osram Rubidium Lamp.

(v) Hyperfine Structure

The hyperfine structure due to the ground state splitting in the rubidium isotopes was poorly resolved in the lines produced by the Osram lamp operating at currents of less than one ampere, as shown in Figure (22). As the current is increased, each hyperfine component broadens and becomes self-reversed rapidly, and the components are not resolved.

The ground state splitting could be observed throughout the temperature range of the radiofrequency lamp. The separation between the components for each isotope was measured at 10°C intervals. The values obtained were:

Rb^{85}: 0.094 ± 0.001 cm.$^{-1}$

Rb^{87}: 0.231 ± 0.002 cm.$^{-1}$

The errors given are the probable errors in the determinations. The precise values are obtained by the methods of radiofrequency spectroscopy and are:

Rb^{85}: 0.1011 cm.$^{-1}$

Rb^{87}: 0.2278 cm.$^{-1}$ (Ochs and Kusch, 1952)

The values obtained in this investigation differ by 7% and 1.4% respectively.

It was observed that the midpoint of the rubidium 85 components shifted to a lower frequency, with respect to the midpoint of the rubidium 87 components, as the rubidium vapour pressure was increased. The shift was approximately proportional to temperature and was 0.00087 cm.$^{-1}$/ °C. In Figure (27) the rubidium 85 components have shifted to a lower frequency in the 7800 A line, but in the 7948 A line are at a higher frequency than the midpoint of the rubidium 87 components. The values of the shift are given in Table (13) and plotted in Figure (28).

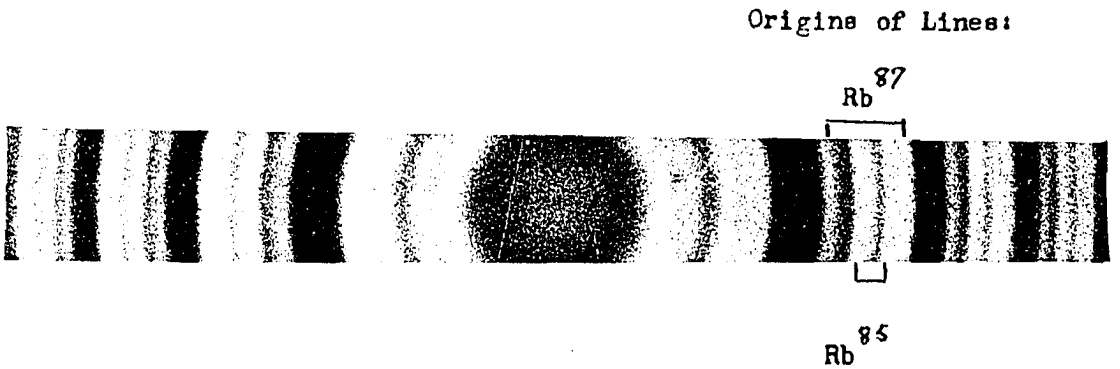

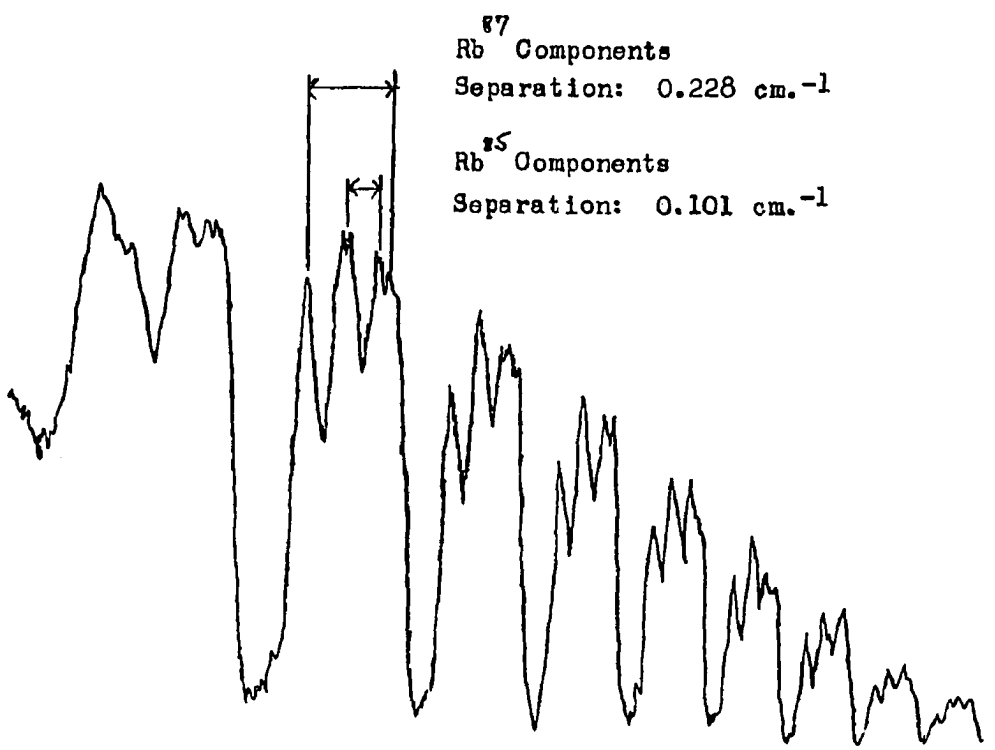

Figure (27a) Photograph of Fringe Pattern and Microphotometer Trace of the Rubidium 7800 Å Component emitted by the Radio-frequency Lamp.

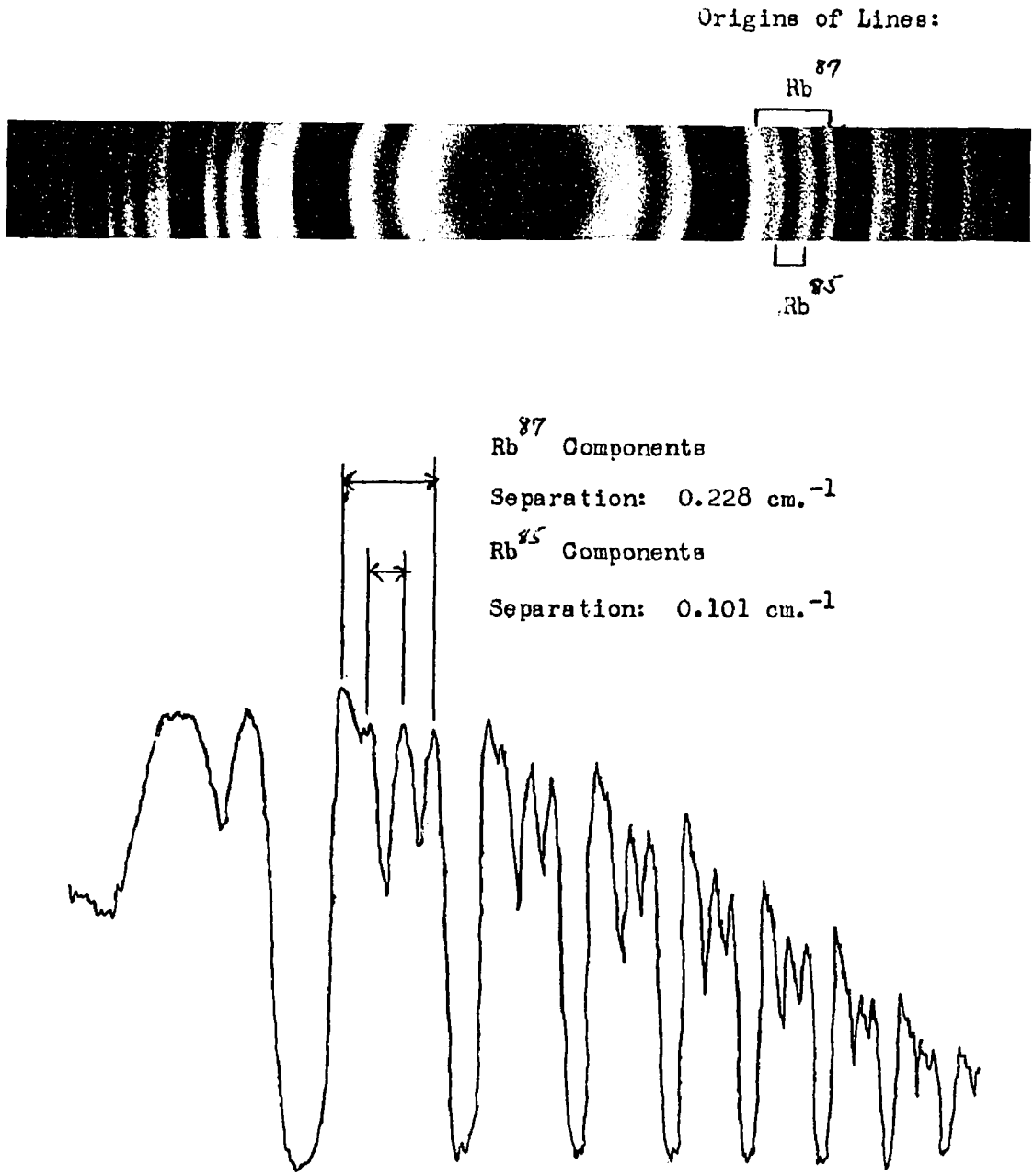

Figure (27b) Photograph of Fringe Pattern and Microphotometer Trace of the Rubidium 7948 Å Component Emitted by the Radio-frequency Lamp.

Table (13)

Position of the Midpoint of the Rubidium 85 Hyperfine Structure Components Relative to the Midpoint of the Rubidium 87 Hyperfine Structure Components

Operating Temp. °C.	Position of 7800 Å Line cm.$^{-1}$	Position of 7948 Å Line cm.$^{-1}$
110	+0.0328	+0.0314
120	+0.0179	+0.0300
130	+0.0115	+0.0241
140	+0.0005	+0.0203
150	+0.0132	+0.0207
160	-0.0121	+0.0118
170	-0.0253	+0.0084
180	-0.0329	+0.0065
190	-0.0435	-0.0147
200	-0.0480	-0.0300
210	-0.0510	-0.0400
220	-0.0580	-0.0370

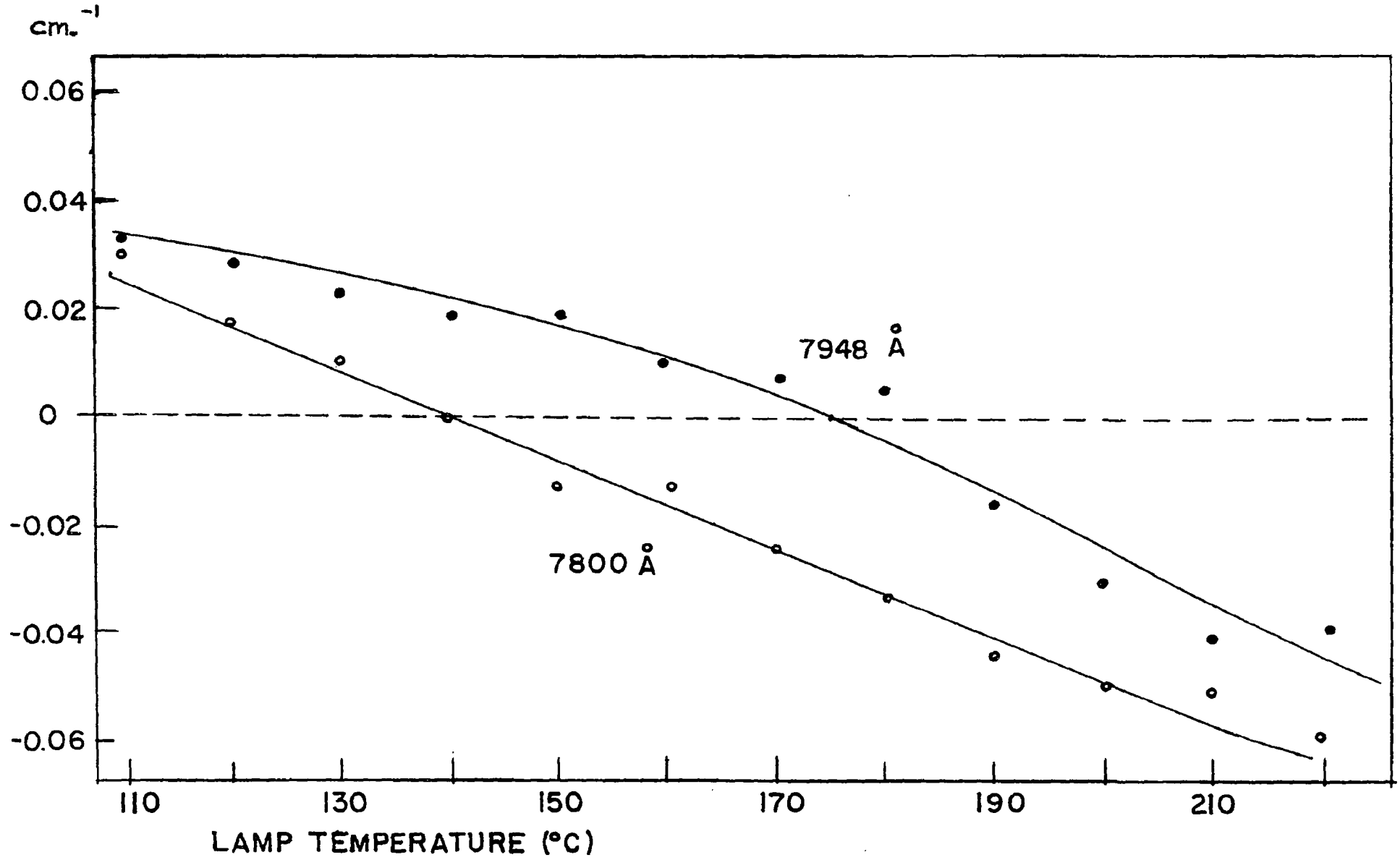

Figure (28) Position of The Midpoint of the Rubidium 85 Hyperfine Structure Components Relative to the Midpoint of the Rubidium 87 Hyperfine Structure Components.

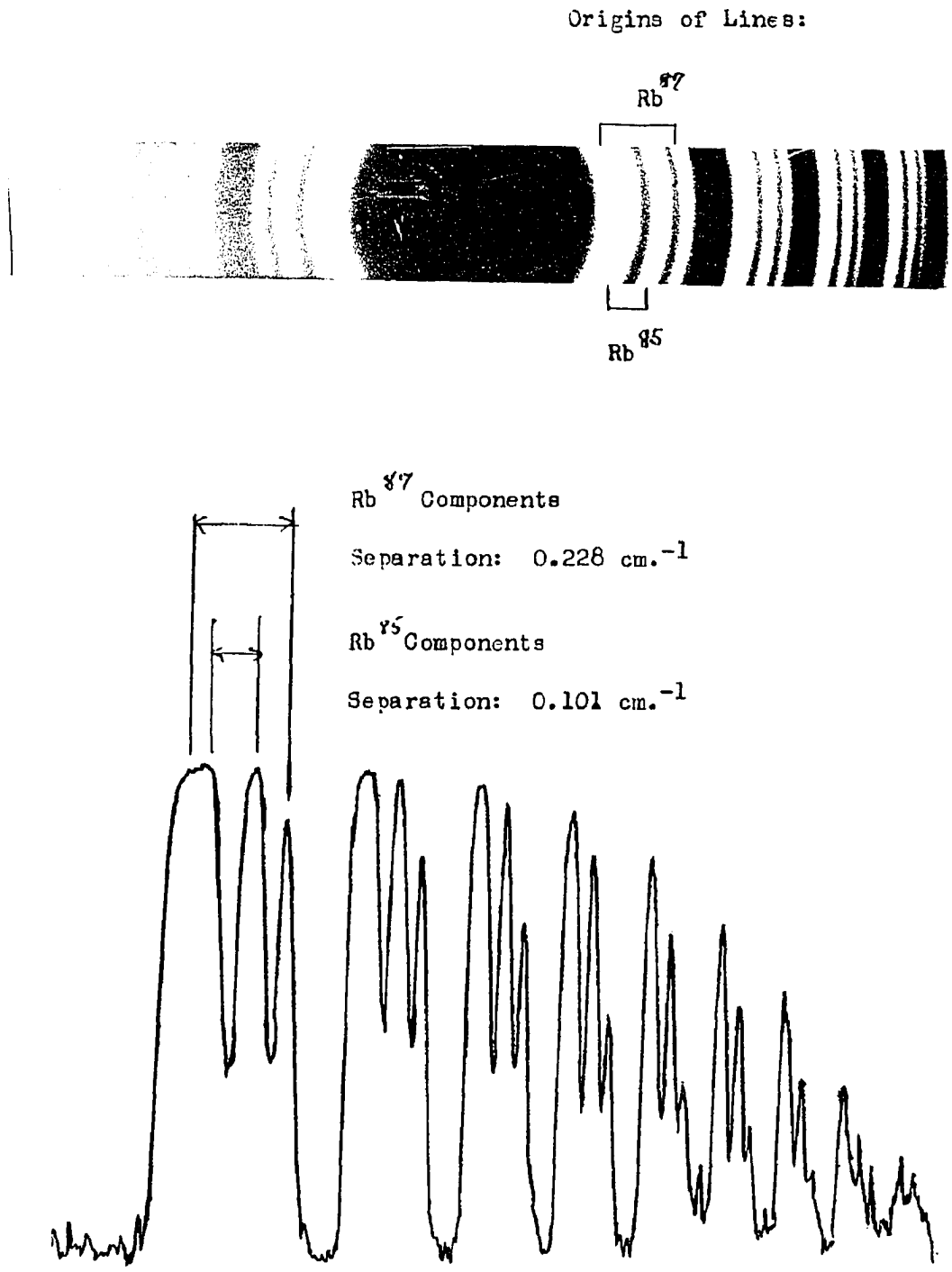

Figure (29) Photograph of Fringe Pattern and Microphotometer Trace of the Rubidium 7948 Å Component Emitted by the Varian Radiofrequency Lamp.

The Broadening of the Potassium and Rubidium Resonance Lines

The theory of self-absorption presented in Chpater II indicates that the square of the separation of the self-reversal peaks should vary either linearly or logarithmically with the absorption parameter when the only non-constant broadening factor is self-absorption. If the square of the peak separations is plotted against the absorption parameter, the slope of the curve is determined by the half-width of the non-absorbed spectral line.

In the case of the Osram lamps, such curves were plotted. It was found that the variation of the square of the peak separations with absorption parameter was more rapid then the linear or logarithmic variation. This indicates that the half-widths of the unabsorbed lines were increasing as the operating current of the lamps was increased. Doppler and Stark broadening are the probable causes of this effect, since an increase in operating current of the lamp brings about an increase in the temperature of the vapour and in the concentration of the ions.

A plot of the experimental values of the squares of the peak separations and the absorption parameters is shown in Figure (30) for the radiofrequency potassium lamp. Curves showing a logarithmic and a linear variation have been drawn, assuming the half-widths of the unabsorbed lines to be 0.11 $cm.^{-1}$ and 0.075 $cm.^{-1}$ for the 7665 Å and 7699 Å lines respectively. The actual form of the variation cannot be determined with certainty, since the region of greatest divergence of the two types of curves lies beyond the range of experimental values. The experimental points appear to give the best fit for the linear variation, which indicates that the distribution function is of the resonance type.

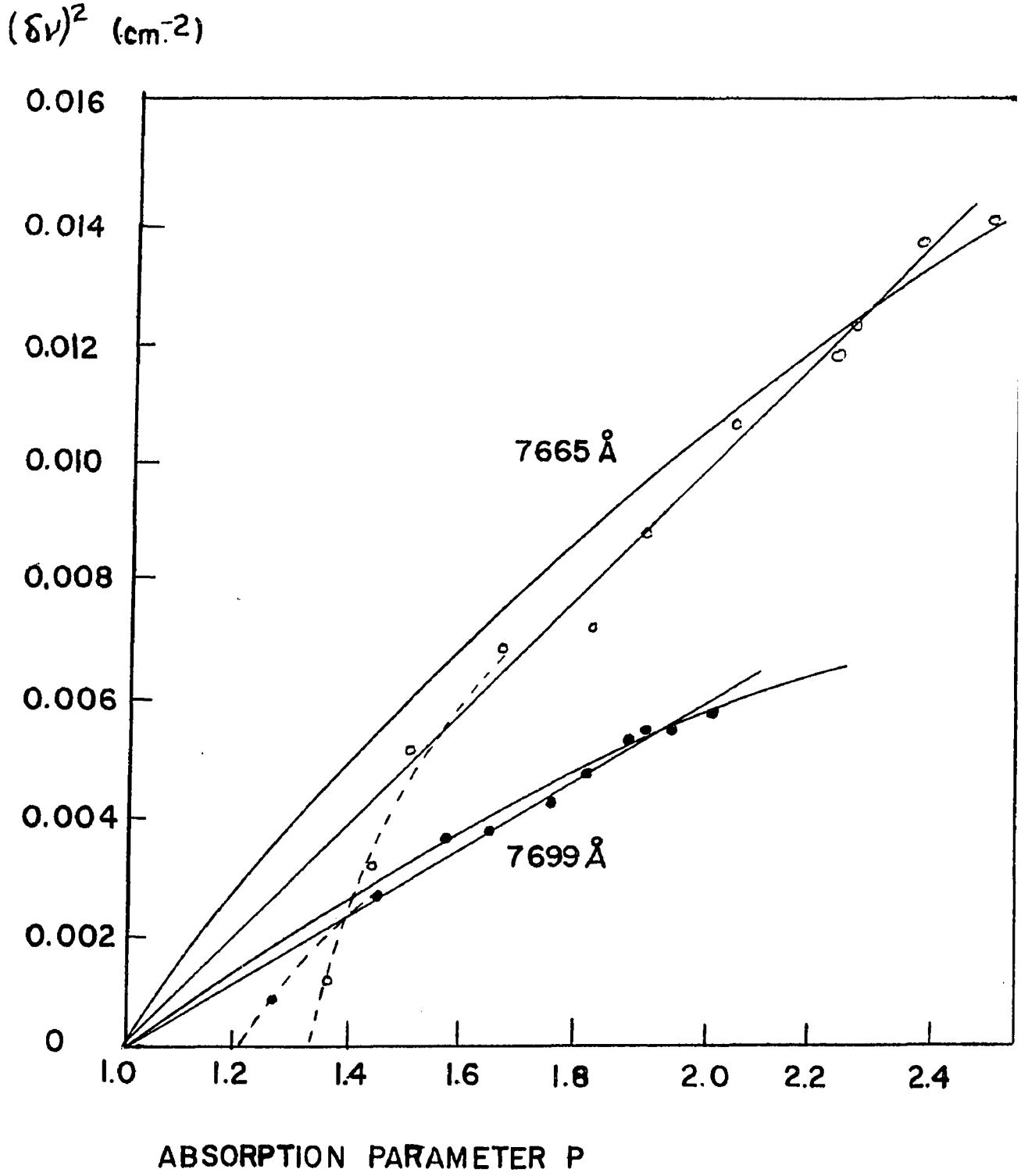

Figure (30) Plot of the Square of Self-Reversal Peak Separations vs. Absorption Parameter in the Radiofrequency Potassium Lamp. The solid curves show linear and logarithmic variations.

However, the downward curvatures for small values of the absorption parameter, indicated by the dashed lines, may be attributed to the influence of a Doppler distribution (Cowan and Dieke, 1948).

The resonance distribution is preserved under collision broadening, and the broadening due to the presence of argon would be nearly constant throughout the range of operating conditions. The half-widths of the spectral lines might be larger than the calculated values, since for relatively low pressures of argon, as used in the radiofrequency lamp, the half-width does not decrease as rapidly as is indicated by the Lorentz theory, which was used in determining the experimental values of the optical collision diameters (Ch'en and Takeo, 1957). Doppler broadening also might be larger than the calculated value, since the temperature of the vapour is not accurately known; the motion of the particles in the radiofrequency field might well produce particle velocities much greater than their thermal velocities. Stark broadening due to argon ions should be considered. This effect would be nearly constant, as is the density of the argon in the lamp.

Resonance broadening due to self-pressure should not appear until the vapour pressure reaches 0.1 mm. Hg, according to the calculated values. For potassium, this occurs at a temperature of 270°C, which was not attained. The vapour pressure of rubidium reaches this value at the higher operating temperatures of the radiofrequency lamp, where a more rapid increase of half-widths was observed.

CONCLUSIONS

Several of the properties of Osram lamps, of the new radiofrequency lamp, and of the Varian radiofrequency lamp were investigated. Measurements of the peak intensities, the integrated intensities, the half-widths, and the degrees of self-reversal were carried out for the resonance lines of potassium and rubidium emitted by these lamps.

It was found that the radiofrequency lamps emit resonance lines whose integrated intensities are twice as large as those emitted by the Osram lamps at their recommended operating currents. In the case of potassium, the new radiofrequency lamp produces non-self-reversed resonance lines with peak intensities greater by a factor of four and half-widths smaller by a factor of two than the Osram lamp. In the case of rubidium, the radiofrequency lamps emit resonance lines with peak intensities greater by a factor of eight and half-widths smaller by a factor of six, with resolved hyperfine structure splitting of the ground states in rubidium 85 and rubidium 87. The hyperfine components of rubidium 85 were found to shift to lower frequencies relative to the components of rubidium 87 as the rubidium vapour pressure increased. This shift was approximately proportional to the temperature which controlled the vapour pressure, and amounted to 0.0009 $cm.^{-1}$ per ^{o}C.

Further improvement in the quality of radiofrequency sources might be attained by confining the discharge to a thin sheet as in the Houtermanns' lamp, and by thermally insulating the discharge tube. It might be worthwhile to investigate the behaviour of such lamps employing other carrier gases as well as argon.

It seems certain that the radiofrequency-excited alkali spectral lamps are very much superior to any commercially available spectral lamps for the purpose of exciting resonance fluorescence in alkali vapours.

BIBLIOGRAPHY

Bell, W. E., Bloom, A. L. and Lynch, J. 1961. Rev. Sci. Instr., 32, 688.

Cario, G. and Lochte-Holtgreven, W. 1927. Zs. Phys. 42, 22.

Chapman, G. D. 1963. M.Sc. Thesis, Assumption University of Windsor.

- - - - - - - - 1964. Private Communication.

Ch' en, S. Y. 1940. Phys, Rev. 58, 884.

- - - - - - - - 1940. Phys. Rev. 58, 1051.

- - - - - - - - and Takeo, M. 1957. Rev. Mod. Phys. 29, 20.

Cowan, R. D. and Dieke, G. H. 1948. Rev. Mod. Phys. 20, 418.

Druyvesteyn, M. J. 1935. Physica 2, 255.

Ermisch, W. and Seiwert, R. 1959. Ann. der Physik, (series 7), 2, 393.

Foley, H. M. 1946. Phys. Rev. 69, 616.

Gerard, V. B. 1962. J. Sci. Instr. 39, 217.

Hoffman, K, and Seiwert, R. 1960 Exper. Tech. der Phys. 8, 161.

Holtsmark, J. 1919. Ann. der Physik, 58, 577.

Houtermanns, F. G. 1932. Zs. Phys. 76, 474.

Hull, G. F. Jr. 1936. Phys. Rev. 50, 1148.

Jackson, D. A. 1928. Proc. Roy. Soc. A121, 432.

- - - - - - - - 1933. Proc. Roy. Soc. A139, 673.

Lloyd, P. E. and Hughes, D. S. 1937. Phys. Rev. 52, 1215.

London, F. 1930. Zs. Phys. 63, 245.

Lorentz, H. A. 1906. Proc. Amst. Acad. 8, 591.

Margenau, H. and Watson, W. W. 1936. Rev. Mod. Phys. 8, 22.

Ochs, S. A. and Kusch, P. 1952. Phys. Rev. 85, 145.

Rae, A. G. A. 1963. Private Communication.

Stone, J. M. 1963. Radiation and Optics, McGraw-Hill Book Co., Inc., 295.

Tolansky, S. 1931. J. Sci. Instr. 8, 223.

Weisskopf, V. F. and Wigner, E. 1930. Zs. Phys. 63, 54.

Weisskopf, V. F. 1932. Zs. Phys. 75, 287.

- - - - - - - - - - - - - - - - - - - 77, 398.

VITA AUCTORIS

1941 - born in Wheatley, Ontario on October 21.

1954-1959 - attended Merlin District High School, Merlin, Ontario, obtaining Senior Matriculation.

1963 - obtained the degree of Bachelor of Science, Honours Physics, from Assumption University of Windsor.

1963 - entered the Faculty of Graduate Studies of the University of Windsor, proceeding toward the degree of Master of Science in Physics.